The Faculty of Biomedical Engineering

Technion

Projects Conference

June 26, 2018

Abstracts

הטכניון - מכון טכנולוגי לישראל / הפקולטה להנדסה ביו-רפואית

TECHNION – Israel Institute Of Technology / Department Of Biomedical Engineering

TECHNION
Israel Institute
of Technology

Dear all,

The Annual Projects Conference in Biomedical Engineering is hosted by the Faculty of Biomedical Engineering at the Technion – Israel Institute of Technology. As the Dean of the Faculty of Biomedical Engineering and as the project course staff, we are pleased and honored to welcome you here.

The conference is hosting 4th year students who are eager to present their year-long projects and to receive feedback from academic researchers, industrial experts, and their peers. These projects implement the medical, engineering, and scientific tools that the students have acquired and developed during their BSc journey in Biomedical Engineering.

The students aim to provide solutions that meet research and development needs in the Biomedical industries and research departments. Through working on their projects, students gained invaluable, hands-on experience. They had to work through technical challenges and adhere to strict standards comparable to those in a real-world setting.
We believe that this hands-on experience engages graduates with the Biomedical industry and/or the wide variety of Biomedical research in a very strong way encouraging multidisciplinary work that is vital to the students' futures.

Additionally, we encourage the students to think out of the box to initiate new solutions and help foster their entrepreneurship skills. Above all, these projects are a key element of the faculty vision which strives to strengthen the long-term cooperation between academia and industry leaders.

In this booklet we are introducing the abstracts of all presented projects. We wish all students rewarding careers and bright futures. We hope that one day they will take an active part in similar projects as professional mentors from both the industry and academia.

Kindest Regards,
Prof. Shulamit Levenberg, Faculty Dean
Prof. Netanel Korin, Course Instructor

List of Abstracts

(1) Barcoded Personalized Cancer Medicine Using Signal Processing

Shira Kasten Serlin[1], Anaelle Yasdi[1], Amit Livneh[1], Avi Schreoder[3] and Yonina Eldar[2]
[1] Department of Biomedical Engineering, Technion - IIT, Haifa, Israel
[2] Department of Electrical Engineering, Technion - IIT, Haifa, Israel
[3] Department of Chemical Engineering, Technion - IIT, Haifa, Israel

(2) Compressed Sensing For Ultrasound Elastography

Karine Eliashiv[1], Neta Zimerman[1], Regen Cohen[2], Grigoriy Zurakhov[1], Amit Livne[1], Yonina Eldar[2]
[1] Department of Biomedical Engineering, Technion - IIT, Haifa, Israel
[2] Department of Electrical Engineering, Technion - IIT, Haifa, Israel

(3) Sparse Beamforming for Plane-Wave Coherent Compounding

Raphael Azriel[1], Adi Apotheker[1], Grigoriy Zurakhov[1], Regev Cohen[2], Yonina Eldar[2]
[1] Department of Biomedical Engineering, Technion - IIT, Haifa, Israel
[2] Department of Electrical Engineering, Technion - IIT, Haifa, Israel

(4) Separation of Contrast Agents from Tissue in Ultrasound Imaging

Liran Taib[1], Daniel Toberman[1], Regev Cohen[2], Oren Solomon[2], Gregory Zorchov[1], Yonina Eldar[2]
[1] Department of Biomedical Engineering, Technion - IIT, Haifa, Israel
[2] Department of Electrical Engineering, Technion - IIT, Haifa, Israel

(5) Malignancy Automatic Detection in Prostate Histopathological Images

Haya Fischer[1,2], Karen Darsa[1], Amit Livneh[1], Edmond Sabo[2,3], Ori Bryt[4]
[1] Department of Biomedical Engineering, Technion – IIT, Haifa, Israel
[2] The Ruth and Bruce Rappaport Faculty of Medicine, Technion – IIT, Haifa, Israel
[3] Carmel Medical Center – Haifa Israel
[4] Department of Electrical Engineering, Technion – IIT, Haifa, Israel

(6) Ultrasound Tomographic Image Reconstruction for Breast Tissue Based on Beam Propagation and Sparse Regularization

Taly Zalman[1], Maor Kakun[1], Regev Cohen[2], Amit Livneh[1], Yonina C. Eldar[2]
[1] Department of Biomedical Engineering, Technion - IIT, Haifa, Israel
[2] Department of Electrical Engineering, Technion - IIT, Haifa, Israel

(7) Automatic Small Bowel Entrance Detection for Wireless Capsule Endoscopy Using Deep Learning

Eran Zvuloni[1], Amit Livneh[1], Eyal Dekel[2]
[1] Department of Biomedical Engineering, Technion - IIT, Haifa, Israel
[2] Medtronic

(8) EEG Analysis with Geometry & Manifold Learning

Nir Habouba[1], Amit Livneh[1], Ronen Talmon[2]
[1] Department of Biomedical Engineering, Technion - IIT, Haifa, Israel
[2] Department of Electrical Engineering, Technion, Signal and Image Processing Lab (SIPL)

(9) Lung Segmentation from Chest X-ray Images for Use in Deep Learning Systems

Eliyahu Rosenfelder[1], Ilai Waimann[1], Amit Livneh[1], Yaron Blinder[2]
[1] Department of Biomedical Engineering, Technion - IIT, Haifa, Israel
[2] Radical AI

(10) Non-Invasive Monitoring of Heart Failure Patients Using Respiratory Signals

Tomer Heitner[1], Noa Markovitch[1], Amit Livneh[1], Shmuel Rispler[2], Amir Landesberg[1]
[1] Department of Biomedical Engineering, Technion - IIT, Haifa, Israel
[2] Rambam Healthcare Campus, Cardiology Department, Haifa, Israel

(11) Focusing Quality in Transcranial MRgFUS by Shifting Phases from Reference Points

Ariel Veler[1], Eyal Abend[1], Oscar Lichtenstein[1], Yoav Levy[2]
[1] Department of Biomedical Engineering, Technion - IIT, Haifa, Israel
[2] INSIGHTEC Ltd, Haifa, Israel

(12) Predictive Model for the Onset of Atrial Fibrillation Events

Yonatan Elul[1], Assaf Shuster[2], Oscar Lichtenstein [1], Alex Bronstein[2], Yael Yaniv[1]
[1] Biomedical Engineering Faculty, Technion - IIT, Haifa, Israel
[2] Computer Science Faculty, Technion - IIT, Haifa, Israel

(13) Prediction of Ventricular Fibrillation Using Heart Rate Variability Indices and Artificial Neural Networks

Noam Keidar[1,4], Gal Eidelsztein[1,4], Ido Weiser-Bitoun[1], Shmuel Rispler[2], Assaf Schuster[3], Alex Bronstein[3], Oscar Lichtenstein[1], Yael Yaniv[1]
[1]Faculty of Biomedical Engineering, Technion IIT
[2]Heart Failure Unit, Department of Cardiology, Rambam Health Care Campus
[3]Computer Science Department, Technion IIT
[4]Faculty of Medicine, Technion IIT

(14) Quantification of the Pulmonary Impedance and the Right Ventricle Contractility

Alon Sideman[1], Efrat Ben-Sadeh[1], Anna Faingersh[1], and Amir Landsberg[1]
[1] Department of Biomedical Engineering, Technion - IIT, Haifa, Israel

(15) Mass Deposition in Cerebral Side Aneurysms

Hadeel Ayoub[1], Mira Vintilescu[1], Mark Epshtein[1], Oscar Lichtenstein[1], Netanel Korin[1]
[1] Department of Biomedical Engineering, Technion - IIT, Haifa, Israel

(16) User Interface Design for a Low-Cost 3D Printed Electro-Mechanical Prosthetic Hand

Shunit Polinsky[1], Yair Herbast[2], Yoav Medan[3]
[1] Department of Biomedical Engineering, Technion - IIT, Haifa, Israel
[2] Department of Mechanical Engineering, Technion - IIT, Haifa, Israel
[3] Haifa3D Founder and Chairman, Visiting Scientist, Technion - IIT, Haifa, Israel

(17) Detecting DNA Mechanical Stretching under Flow

Ali Hilo[1], Rawaa Ayoub[1], Yathreb Asaad[1], Maria Khoury[1], Netanel Korin[1]
[1] Department of Biomedical Engineering, Technion – IIT, Haifa, Israel

(18) Low-Cost 3D Printing for Tissue Engineering

Dana Azagury[1], Moran Moradi[1], Ariel Szklanny[1], Maria Khoury[1], Shulamit Levenberg[1]
[1] Department of Biomedical Engineering, Technion – IIT, Haifa, Israel

(19) Investigation of Particles Deposition Using a 3D Bronchial Airway Model

Nofar Azulay[1], Eyal Habif[1], Shani Elias-Kirma[1], Maria Khoury[1], Josue Sznitman[1]
[1] Department of Biomedical Engineering, Technion – IIT, Haifa, Israel

(20) Utilizing 3D Printing for the Fabrication of Precision Scaffolds for Spinal Cord Injury Repair

Noah Michael[1], Tsemach Bar-Mucha[1], Idan Redenski[1], Ben Kaplan[1], and Shulamit Levenberg[1]
[1] Department of Biomedical Engineering, Technion - IIT, Haifa, Israel

(21) Double-Network Hydrogels for Cartilage Repair

Liaura Ifergan[1], Sapir Cohen[1], Haneen Simaan-Yameen[1], Tamara Birman[1], Olga Kossover[1], Dror Seliktar[1]
[1] Department of Biomedical Engineering, Technion – IIT, Haifa, Israel

(22) Nano-technology for Methylation Site Detection

Tal Elmalich[1], Chen Torfstein[1], Amit Meller[1]
[1] Department of Biomedical Engineering, Technion - IIT, Haifa, Israel

(23) 3D Localization Microscopy by PSF Engineering in Live U2OS Cell Line

Maisa Nasser[1], Reem Shalaata[1], Tal Naor[1,2], Yoav Shechtman[1,2]
[1] Department of Biomedical Engineering, Technion - IIT, Haifa, Israel
[2] Lorry Lokey Interdisciplinary Center for Life Sciences and Engineering, Technion - IIT, Haifa, Israel

(1)

Barcoded Personalized Cancer Medicine Using Signal Processing

Shira Kasten Serlin[1], Anaelle Yasdi[1], Amit Livneh[1], Avi Schreoder[3] and Yonina Eldar[2]

[1] Department of Biomedical Engineering, Technion - IIT, Haifa, Israel
[2] Department of Electrical Engineering, Technion - IIT, Haifa, Israel
[3] Department of Chemical Engineering, Technion - IIT, Haifa, Israel

Introduction: Cancer is a leading cause of death in the Western world. Choosing the best drug for the individual patient, at the right time, is crucial for the success of the treatment. Despite scientific and medical advances many cancer patients are prescribed the wrong medication. This paper introduces a new diagnostic imaging method based on image processing algorithms for determining the suitability of specific anticancer drugs to a specific patient – before treatment even begins. Liposomes, vesicles with an inner aqueous core surrounded by a lipid bilayer, are clinically approved drug carriers accumulate preferentially in solid tumors. A current technic using Genetic Barcoding can identify medication effectiveness however is costly, time consuming and not practical for wide use. Our image processing technic introduces a new cost-effective approach to archiving this goal.

Methods: The approach is based on three-color fluorescent markers testifying on cell location, viability and the treatment by medication. Cancer cells were injected subcutaneously to three mice. Drug-loaded fluorescent liposomes were injected intravenously into two mice (One for control). The tumor was extracted, and the tissue was paraffin embedded. Those paraffin-embedded slides were stained by markers for cell location (cell nuclei), viability (Caspase-3 which is activated in the apoptotic cell) and the treatment by medication (liposomes). Auto-fluorescence is a known problem in tissue image analysis. In order to overcome this, we used in-vitro images (free of Auto-fluorescence) as a reference identifying the desired signal to build the filtering algorithm according to the noise profile. For automatic analysis of the scanned images, a Matlab image processing software solution was developed. The analysis made by the software includes: Graphical User Interface for selecting the non-necrotic areas, filtering of scanned Images, nuclei segmentation and counting the apoptotic and live drug-treated cells for determining the efficiency. Two methods were compared. The first based on finding liposomes center of mass and attribution to the nearest cell. The second based on searching signals around the cell nuclei.

Results: The tool successfully identified the apoptotic drug-treated cells and showed results of effectiveness. Apoptotic signal normalized by area in the treated slide was 15 times higher than the control slide. The number of liposomes accumulation in the treated slide was 40 times of that in the control slide (noise). For validation results from representative areas were compared to manual analysis.

Conclusion: Our Image Processing approach offers an automatic cost-effective addition to the current personalized cancer medicine technic. The software tool help physician predicts patient response to medication and help with histology analysis and reducing the human error factor.

Keywords: Image processing, cell segmentation, immunofluorescence analysis, personalized medicine

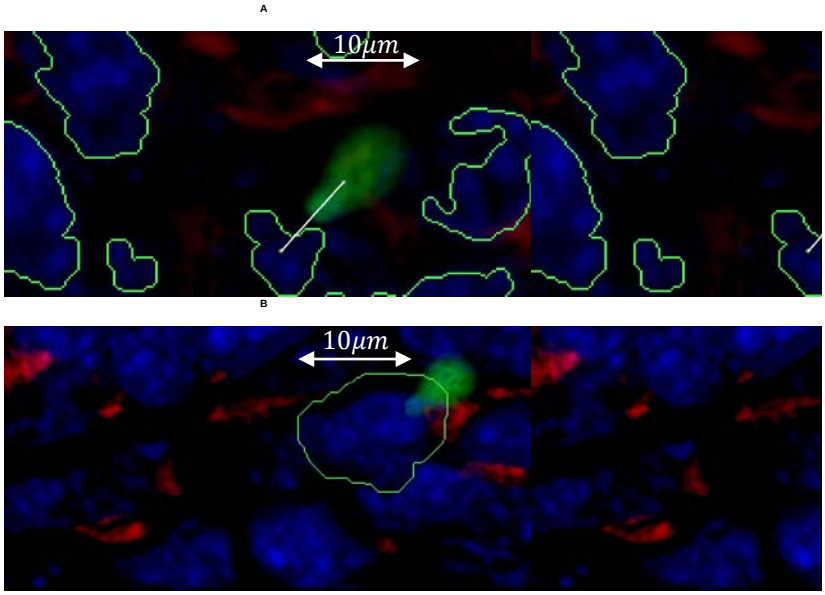

Figure 1: filtered treated slide. cell nuclei (blue), apoptotic signal (red), liposomes (green), Two methods were compared. A. first method based on finding liposomes center of mass and attribution to the nearest cell. B. Second method based on searching signals around the cell nuclei.

(2)

Compressed Sensing for Ultrasound Elastography

Karine Eliashiv[1], Neta Zimerman[1], Regev Cohen[2], Grigoriy Zurakhov[1], Amit Livne[1], Yonina Eldar[2]

[1]Department of Biomedical Engineering, Technion - IIT, Haifa, Israel
[2]Department of Electrical Engineering, Technion - IIT, Haifa, Israel

Introduction**:** Ultrasound Elastography was developed in the 1990's, to map tissue stiffness and replace the palpation performed by clinicians. It is a medical imaging modality that maps the elastic properties of soft tissue, and thus provides diagnostic information about the presence or status of disease. Acquiring the elastography image requires multiple data and high computational complexity. In the first stage of the process, mechanical impulse is applied, creating a lateral plane of shear waves, propagates through the tissue. in the second stage, elements transduce ultrasonic waves creating constructive interference. This process is called static focusing (Beam forming) in which several pulses are applied to measure the shear wave propagation through the tissue. Considering the great number of pulses and probe elements, the acquire time is relatively long, and complicates the development of 3D applications. This fact highlights the motivation for developing new algorithm for efficiently acquiring and reconstructing a signal from fewer samples. This paper introduces a new method for efficiently acquire elastography image by reducing transmissions, based on compressed sensing principals.

Methods: A phantom containing cylindrical lesions with different elastic modulus, was scanned using standard shear wave elastography. Signal was processed to create an ultrasonic image per transmission, following by a velocity estimation process. In standard elastography methods, autocorrelation of pulses is applied to estimate the propagation velocity throughout the tissue and obtaining an elastography image.
A reduction algorithm was developed, which under stationary signal assumptions can reduce the amount of data without affecting autocorrelation result. Algorithm was implemented into a standard velocity estimation process, with different percentage of pulses reduction. A map of Young's modulus was calculated to create the elastography image, by using the direct relation to medium shear wave velocity, assuming biological tissues density.

Results: Physician analyze elastography image by observing object elasticity and shape, to determine prognosis. Elastography images followed by pulses reduction showed that

lesion shape and average elasticity modulus are preserved after reduction of 47% of pulses or less, with a relative error of 1.4% compared to reference image. Although mathematical model indicated reduction is possible up to 71%, results showed that reduction of more than 47% pulses is not applicable, due to image distortion. In high reduction rate images, lesion is not detectable and average elasticity modulus has high relative error, up to 23%.

Conclusions: The results demonstrate feasibility to reconstruct elastography images with only 53% of original pulses, reducing data amount by approximately half. Images produced by the reduction algorithm could be used for prognosis in clinical purpose, with the advantages of reducing process time, data rate and improving accuracy of lesion location. However, the reduction rate is limited, based on standard elastography wave frequencies, reducing more than 47% of pulses, causes aliasing phenomenon and lesion is not detectable. The reduction algorithm can be also implemented on probe elements to further improve data rate and process time.

Keyword: Ultrasound Elastography, Compressed sensing, Autocorrelation.

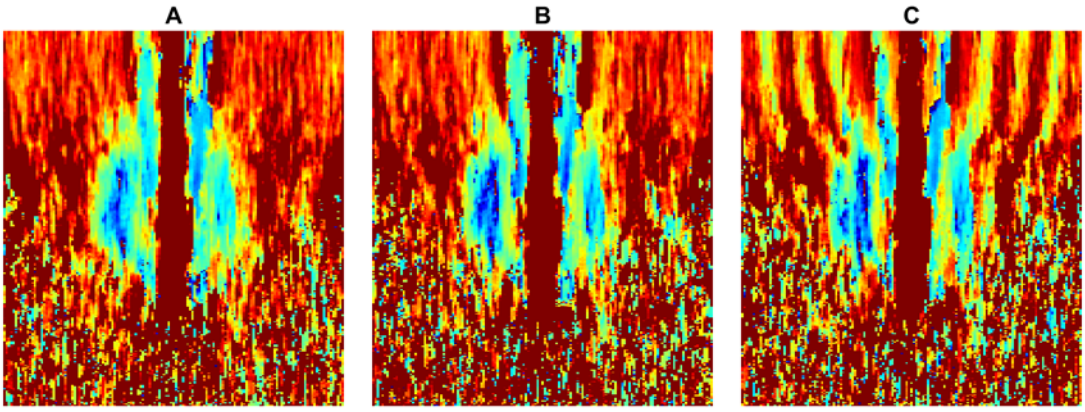

Figure 1: Elastography images showing map of Young's modulus through scanned phantom, lesion circular section in the center. A. Reference image, no pulses reduction. B. Image reconstructed following reduction of 47% pules. C. Image reconstructed following reduction of 56% pules

(3)

Sparse Beamforming for Plane-Wave Coherent Compounding

Raphael Azriel [1], Adi Apotheker [1], Grigoriy Zurakhov [1], Regev Cohen [2], Yonina Eldar[2]

[1] Department of Biomedical Engineering, Technion - IIT, Haifa, Israel
[2] Department of Electrical Engineering, Technion - IIT, Haifa, Israel

Introduction: Ultrafast imaging based on coherent plane-wave compounding is one of the most important recent developments in medical ultrasound. It consists of coherently compounding several tilted plane-wave frames which improves image quality and allows for much faster image acquisition. However, it relies on the standard delay and sum (DAS) beamforming which exhibits limited image resolution and contrast. Image quality can be improved by increasing the number of titled plane-waves or by increasing the number of transducer elements (larger aperture). While the first solution decreases the frame-rate, the latter increases the data size and the system cost. Here, by sparse convolutional beamforming algorithm (SCOBA) we reduce the number of receiving channels while producing ultrafast high-quality images.

Methods: We introduce a non-linear beamforming technique for coherent plane-wave compounding which allows a notable element reduction while providing B-mode images with enhanced resolution and contrast at an ultrafast frame rate. The proposed beamformer is based on a sparse array geometry, composed of two uniform linear arrays with different spacing, and requires elements to attain the same beam pattern as of DAS operating on uniformly spaced elements.

Results: The performance of the proposed method is verified using the PICMUS datasets. The following are results on in vivo data of a carotid artery. Panel (a) shows the result of coherent plane-wave compounding with DAS beamforming applied on 128 elements. Panel (b) shows the result of coherent plane-wave compounding with the

proposed sparse beamforming by SCOBA method applied on 43 out of 128 (~33%) transducer elements with dynamic apodization.

Conclusions: Sparse Beamforming allows for ultrafast imaging with improved image quality while reducing the number of receiving channels.

Keywords: SCOBA, Beamforming, Elements, Dilution

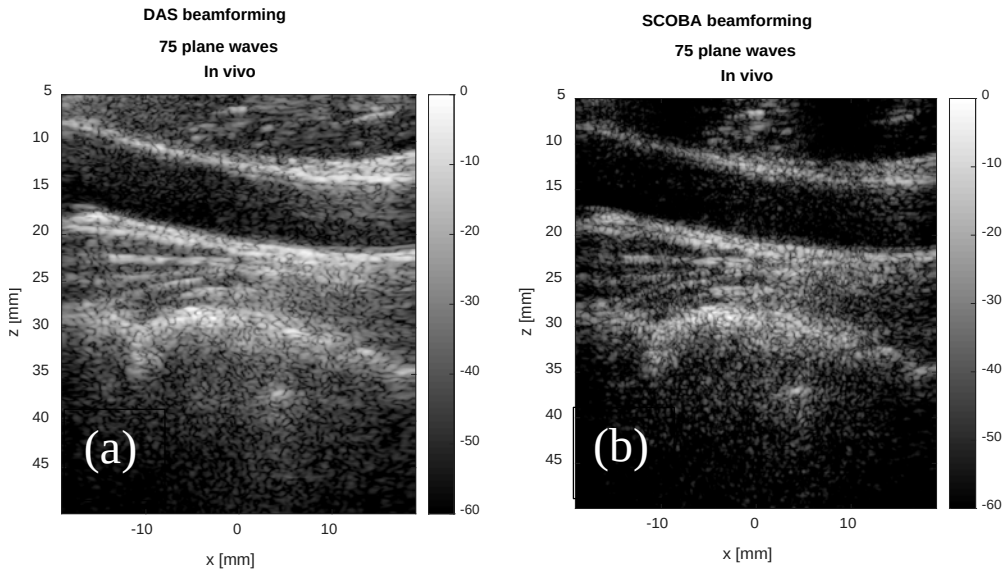

Figure 1: (a) DAS beamforming applied on 128 elements. (b) Sparse beamforming applied on 43 out of 128 elements.

(4)

Separation of Contrast Agents from Tissue in Ultrasound Imaging

Liran Taib[1], Daniel Toberman[1], Regev Cohen[2], Oren Solomon[2], Gregory Zorchov[1], Yonina Eldar[2]

[1] Department of Biomedical Engineering, Technion - IIT, Haifa, Israel
[2] Department of Electrical Engineering, Technion - IIT, Haifa, Israel

Introduction: A dominant characteristic of malignant tumors is that often they encourage angiogenesis in the tissue surrounding them. This allows an amplified source of nutrients to the tumor. One method of detecting malignant tumors is to identify enhanced angiogenesis. Contrast enhanced ultrasound (CEUS) imaging enables vascular visualization with high contrast using inert microbubbles (MBs), injected into the bloodstream. CEUS processing requires separating tissue signal from the MB signal, prior to subsequent processing. Several separation techniques exist, such as the well-known SVD filtering. However, selection of the cutoff threshold in SVD is data-dependent and wrong choice often results in noisy or cluttered CEUS signals. Here, we propose a low-rank and sparse (L+S) decomposition to solve the separation problem, which alleviates the need to a-priori estimate the rank of the tissue signal matrix and is considered to be robust in the presence of sparse outliers (MBs). We then unfold the corresponding iterative algorithm via recently developed deep-learning techniques to improve its convergence speed, reconstruction quality and reduce its computational complexity.

Methods: CEUS scan of two rat brains were acquired using a Verasonics scanner, courtesy of the center for biomedical imaging research, Tsinghua University. After demodulation and beamforming of 100 CEUS frames, the complex analytical clip is modeled as a sum of a low-rank (tissue) and sparse matrix (MBs). Next, we solve an optimization problem, based on the L+S decomposition, using the fast iterative shrinkage/thresholding algorithm (FISTA/ISTA). We later unfold the iterative scheme of ISTA over a few iterations, where each iteration is a layer in a deep network. We train the network on the FISTA recovery obtained from the experimental data from the first mouse. We test the performance of the network on the second mouse and compare it with the naive SVD decomposition and FISTA.

Results: We achieved a comparable image through FISTA approximation (Figure 1). Significant noise reduction is noticeable, yet image data is not lost.

Conclusions: The following results show the benefits of using an L+S decomposition over SVD. Panel (a) shows the CEUS signal after performing a naïve SVD decomposition (attained from keeping the 50 smallest eigenvalues out of 100). Panel (b) shows the CEUS signal obtained from the FISTA minimization of the L+S decomposition over 20000 iterations. Both images have a dynamic range of 120dB, and are obtained by estimating the pixelwise variance from the separated CEUS movie. The L+S decomposition shows a cleaner and sharper image of the vasculature, as compared with the naïve SVD approach, due to its robustness to sparse outliers and noise handling.

Keywords: Ultrasound, Deep Learning, ISTA, Vascular Visualization

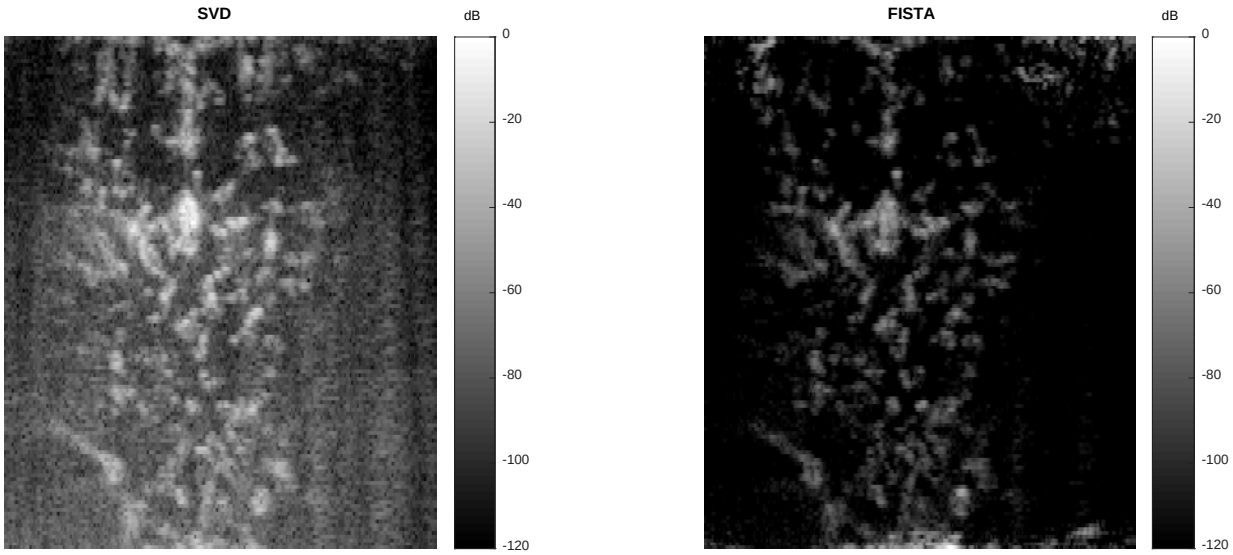

(a) (b)

Figure 1: Panel (a) shows the CEUS signal after performing a naïve SVD decomposition in dB scale with dynamic range of 120dB. Panel (b) shows the CEUS signal obtained from the FISTA minimization of the L+S decomposition in dB scale with dynamic range of 120dB.

(5)

Malignancy Automatic Detection in Prostate Histopathological Images

Haya Fischer[1,2], Karen Darsa[1], Amit Livneh[1], Edmond Sabo[2,3], Ori Bryt[4]

[1] Department of Biomedical Engineering, Technion – IIT, Haifa, Israel
[2] The Ruth and Bruce Rappaport Faculty of Medicine, Technion – IIT, Haifa, Israel
[3] Carmel Medical Center – Haifa Israel
[4] Department of Electrical Engineering, Technion – IIT, Haifa, Israel

Introduction: Prostate cancer is the most common cancer in men in the United States. It is the second leading cause of death from cancer in men[1]. Currently, the diagnosis is made by a pathologist examination of histopathological biopsy images under the microscope. Most pathologists work under a significant amount of load due to multiple examinations of histological specimens daily. This overload may lead to significant delays in diagnosis time, causing stress to the patient and increasing the pathologist's fatigue. It may also lead to increases in error. In our project, the main goal is to develop a tool that allows automatic and fast detection of prostate cancer in histopathological images, in order to help pathologists to significantly reduce pathologists' examinations number and the time to diagnosis.

Methods: Our analysis is based on texture features extracted using Wavelets and Local Binary Patterns (LBP). A Multi-Resolution approach was chosen to mimic the pathologist diagnosis technique for biopsy images. Our data consisted of 790 images which were equally divided to two groups of benign and malignant specimens. At first, Wavelet coefficients were used for classification of the images, as this is a well-known Multi-Resolution decomposition. In order to use the LBP decomposition in a multi-resolution approach, a Gaussian Pyramid was built, and the LBP features were extracted for every pyramid level. This analysis was made separately on the grayscale channels of the RGB image. As a classification method, we chose a supervised learning algorithm – Logistic Regression. A cross-validation technique was used, while the training set included 85% of the images and the test set the remaining 15%. During the training phase, the most relevant features were selected by the algorithm for each resolution and the same subset of features was later used for evaluating the classification on the test set. A block diagram of the project stages appears in Figure 1.

[1] According to The National Cancer Institute, USA

Results: Success was defined as an average between specificity and sensitivity scores (Figure 1). A 96% accuracy was achieved on the blue channel, using 17 features and 4 pyramid levels. Differences of 2% were found between different color channels in RGB.

Conclusions: The highest score achieved was in the Blue channel. The H&E staining (Hematoxylin & Eosin) marks the epithelial cells' nuclei around the prostate glands. When comparing benign and malignant glands, nucleoli are more prominent in the latter, therefore causing the blue staining (Hematoloxylin) to be protuberant. When combining Wavelets and LBP features, the LBP features were found to be more significant in the binary classification. Overall, the extracted features provided generalization on the independent testing set, leading to high accuracy results. Based on the results achieved, the algorithm may be used as a Decision Support System for clinical use in the future.

Keywords: Prostate cancer, Wavelets, LBP, histopathological images

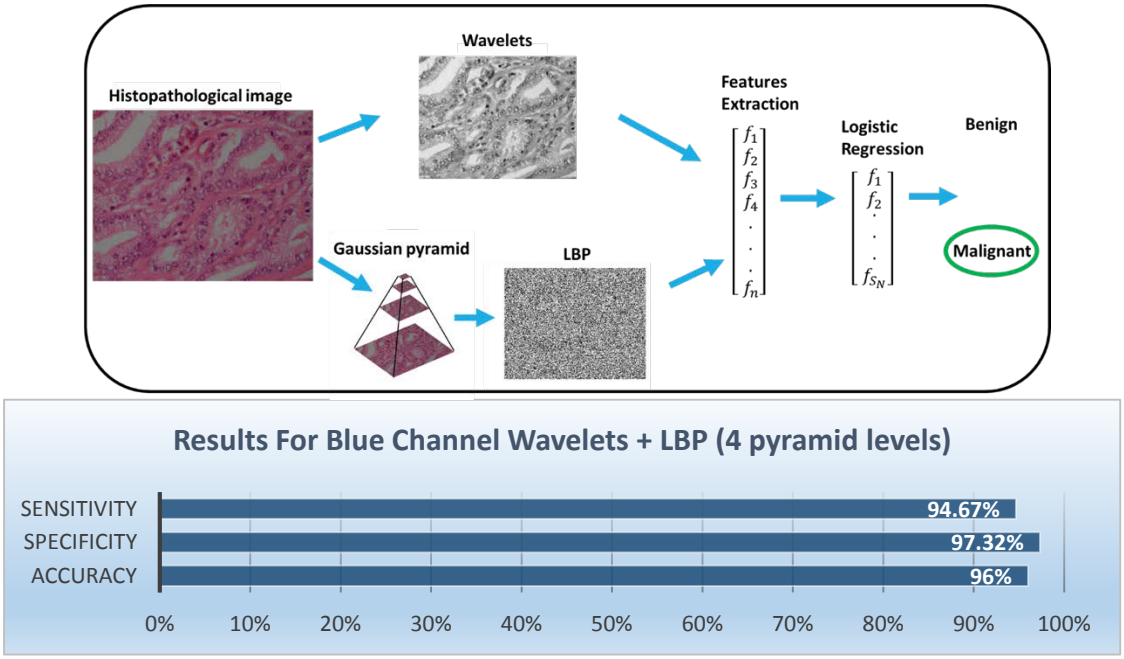

Figure 1: A block diagram of project's workflow & highest results achieved.

(6)

Ultrasound Tomographic Image Reconstruction for Breast Tissue Based on Beam Propagation and Spars Regularization

Taly Zalman[1], Maor Kakun[1], Regev Cohen[2], Amit Livneh[1], Yonina C. Eldar[2]

[1] Department of Biomedical Engineering, Technion - IIT, Haifa, Israel
[2] Department of Electrical Engineering, Technion - IIT, Haifa, Israel

Introduction: Ultrasound Computed Tomography (USCT) is a medical imagining method for breast cancer diagnosis. In this method, image reconstruction is based on the sound-waves distorted by tissue characteristics, such as refractive indexes. Due to the relatively low energy of ultrasound (US) waves, scattering effects are dominant. Current reconstruction methods neglect these effects, hence, assume US waves propagate linearly as straight-rays. Non-linear forward modeling may provide a more accurate interpretation of the data, but further increase the computational burden. In this project we present an iterative reconstruction method that combines a non-linear forward model with sparse regularizer, which allows for an efficient reconstruction along with data reduction.

Methods: Here we present a new forward model based on Beam Propagation Method (BPM), adopted from optics. BPM is a *non-linear* modeling technique for electromagnetic waves propagation in inhomogeneous medium. BPM allows to obtain wave-field via alternating evaluation of diffraction and refraction steps handled in the Fourier and space domains, respectively. Based on this model, we formulated an optimization problem, in respect to the refractive indexes. In order to solve this problem, a gradient based optimization algorithm was used. Since breast tissue is a relatively homogenous medium, the reconstructed data is assumed to be sparse. Therefore, we implemented a sparsity-derived regularizer, FISTA, to the solution. To overcome the computational burden, we used stochastic gradient algorithm and reconstructed with partial data.

Results: We applied the proposed recovery algorithm on a simulated breast tissue USCT data. We compared both SNR and blurring of the reconstructed images and the linear reconstruction presented in the literature (originated from the same data) with the simulation. We infer that the proposed method resulted in an improved image quality of SNR=39.16. Moreover, stochastic gradient resulted in a shorter computation time with minimal image corruption, SNR= 37.36. (see figure 1)

Conclusions:

- USCT reconstruction based on a non-linear forward model, BPM, produces high quality images.
- The sparsity-based optimization algorithms showed improvement in the reconstructed images.
- Stochastic gradient and the non-linear forward model allowed for a faster, more efficient recovery.
- The algorithm is sensitive to the set of parameters used for the recovery, such as step size, regularization coefficient, and the initial image guess.

Keywords: Ultrasound Computed Tomography, Beam Propagation Method, Sparse Reconstruction, FISTA, Stochastic Proximal Gradient.

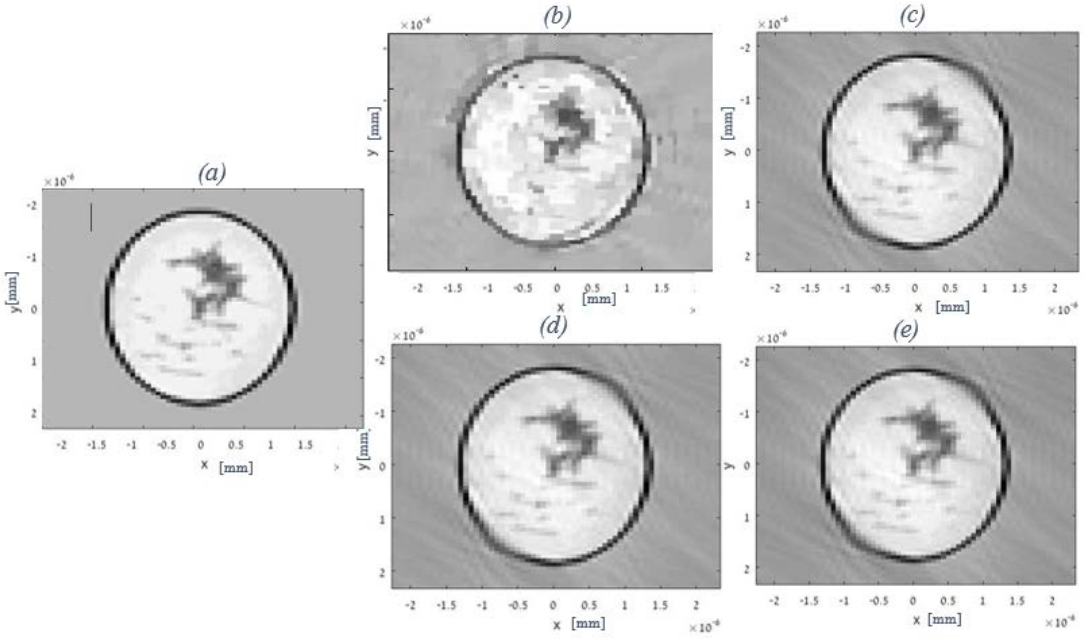

Figure 1: (a) simulated breast tissue image. (b) reconstructed image using linear model (from the literature) (c). reconstructed image using gradient descent SNR=36.38. (d) reconstructed image using FISTA SNR=39.16. (e) reconstructed image using stochastic gradient SNR=37.36 (45 views).

(7)

Automatic Small Bowel Entrance Detection for Wireless Capsule Endoscopy Using Deep Learning

Eran Zvuloni[1], Amit Livneh[1], Eyal Dekel[2]

[1] Department of Biomedical Engineering, Technion - IIT, Haifa, Israel
[2] Medtronic

Introduction: Diagnosis of diseases (e.g. Crohn's disease, Iron Deficiency Anemia, Colorectal Cancer, etc.) within the Gastrointestinal tract (GI tract), mainly along the Small Bowel (SB), is a common procedure among gastroenterologists. Today, Wireless Capsule Endoscopy (WCE) is a leading technology that is accountable for these SB pathologies analyses. While WCE scans the GI tract, the capsule provides comprehensive images of the entire digestive system, yet, most of this data is collected from areas that have minor clinical significance for these diagnoses. Therefore, automated segmentation of the SB within the GI tract WCE video is essential for efficient diagnosis. This reduces the required time of reviewing and analyzing the entire data frame by frame. In this work, we detect the proximal edge of the SB in WCE videos, by autonomously marking its entrance after the capsule is leaving the stomach.

Methods: We use deep learning with Convolutional Neural Networks (CNNs) to classify big sets of video frames that are taken from WCE procedures. Each video includes a "true transition" frame marked by a physician, which indicates the SB entrance. Images are divided into train, test and validation sets. The CNNs that are used are state of the art networks that were pretrained on ImageNet database. These are going through additional training and fine-tuning with our bowel data. During the training the images are classified into two categories: before the entrance of the SB ("PreSB") and after the entrance ("SB") (see figure 1A). After training is completed, we extract signals of frames classifications from the CNN (see figure 1B). Then, we apply signal processing with moving average filtering to detect the desirable landmarks of the videos (see figure 1C).

Results: Microsoft's Resnet V1_50 provided 98.8% accuracy of classifying the video frames to the categories of PreSB and SB. Train, test and validation sets revealed medians of 0.01, 0.02 and 0.05 minutes of absolute time difference respectively between the physician's true transition marks and the landmark algorithm detections.

Conclusions: SB entrance was detected accurately (median of 0.05 minutes out of average of 10 hours per case – 0.008% precision resolution) based on the validation set. The developed system can be assimilated on series of preprocessing algorithms that are applied on the WCE captured videos, as a pre-stage to be handed over to the physician

for diagnosis. Algorithm outliers included patients with contaminated stomach and unusual bowels motility of the capsule inside the GI tract. Further future work may be performed, while these outliers can be used as prior data.

Keywords: Wireless Capsule Endoscopy, Small Bowel, Deep Learning, Convolutional Neural Networks, Autonomous Detection.

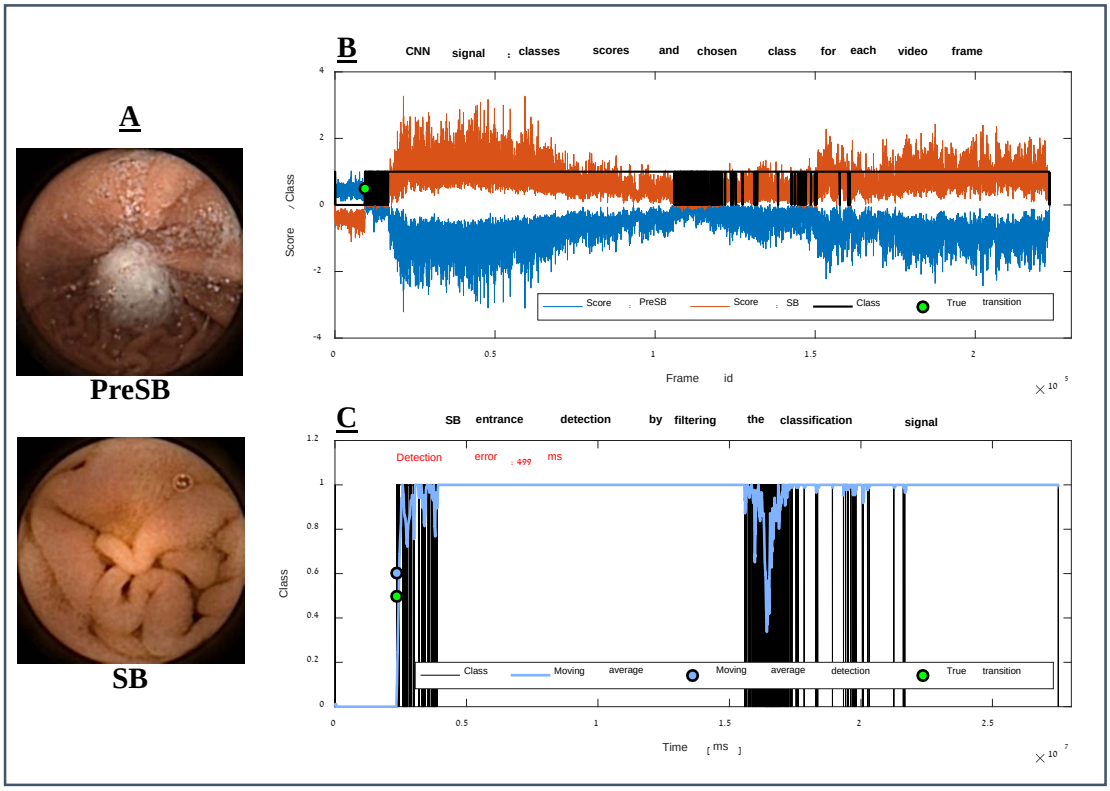

Figure 1: Convolutional Neural Network (CNN) results for detection of the Small Bowel (SB) entrance: (A) Examples of images taken from the bowel data – image taken before the SB entrance ("PreSB") on top, and within the SB ("SB") on bottom. (B) CNN signal extracted from the trained network. Scores for both classes and the classifications (0 for PreSB and 1 for SB) are shown for each video frame. True transition marked by a physician is shown as well. (C) Signal processing with moving average filter is applied on the classification signal from figure 1B to detect the transition. 499ms separate between the true transition and the algorithm detection.

(8)

EEG Analysis with Geometry & Manifold Learning

Nir Habouba[1], Amit Livneh[1], Ronen Talmon[2]

[1] Department of Biomedical Engineering, Technion - IIT, Haifa, Israel
[2] Department of Electrical Engineering, Technion, Signal and Image Processing Lab (SIPL)

Introduction: Nowadays, Brain-computer interface (BCI) based on Electroencephalography (EEG) is of a great interest among neurologists and scientists all over the world and is well studied in the literature for its ability to detect brain functionality \ states. One of the main challenges in EEG analysis is to overcome the variability in the acquired signals from different subjects or even from same subject on different times. That is in addition to EEGs natural not stationary noisy form. Motivated by the idea of designing and calibrating a universal system for brain damage diagnosis, in this project we proposing an approach for analyze EEG signals using Riemannian geometry framework.

Methods: We use Symmetric Positive Definite (SPD) matrices to capture the manifold\geometry structure of the data, which usually embedded in high dimensional space. Specifically, we use covariance matrices that provide a nonlinear low dimensional representation of the raw data. Moreover, to circumvent the high variability of the EEG signals we use Parallel Transport (PT) which is a domain adaptation method for smooth manifold.

Results: To demonstrate our methods we use data from Physionet [https://www.physionet.org/ pn4/eegmmidb/] collected by "Wadsworth" center- New York State Department of Health in cooperate with Albany University. 109 healthy subjects performed (each) 6 motor and\or mental tasks ([1]eyes open, [2]eyes closed, [3]open and close left or right feet, [4]imagine opening and closing left or right fist, [5]open and close both fists or both feet, [6]imagine opening and closing both fists or both feet) which were obtained by 64 EEG sensors. Tasks 3, 4, 5, and 6 were repeated 3 times. Figure 1(a) presents low dimensional representation of the acquired data using the common approach based on SPD matrices. We observe that the different tasks are not separated. Figure 1(b) present the low dimensional representation obtained by our approach. We observe a separation between the eyes open, eyes closed tasks and all other tasks (which are still not separated).

Conclusions: Using the Riemannian geometry we presented an algorithm for analyzing EEG signals. The results demonstrate possible approach to identify brain functionality \ states. The distinct advantage of the presented methods is that it does not require prior model knowledge or strong assumptions on the nature of the data, therefore it is not

limited to the field of EEG signals. We believe that our approach is a cornerstone toward designing a universal system for diagnose brain damage.

Keywords: EEG, Riemannian geometry, Diffusion Maps, Symmetric Positive Definite (SPD), Parallel Transport (PT).

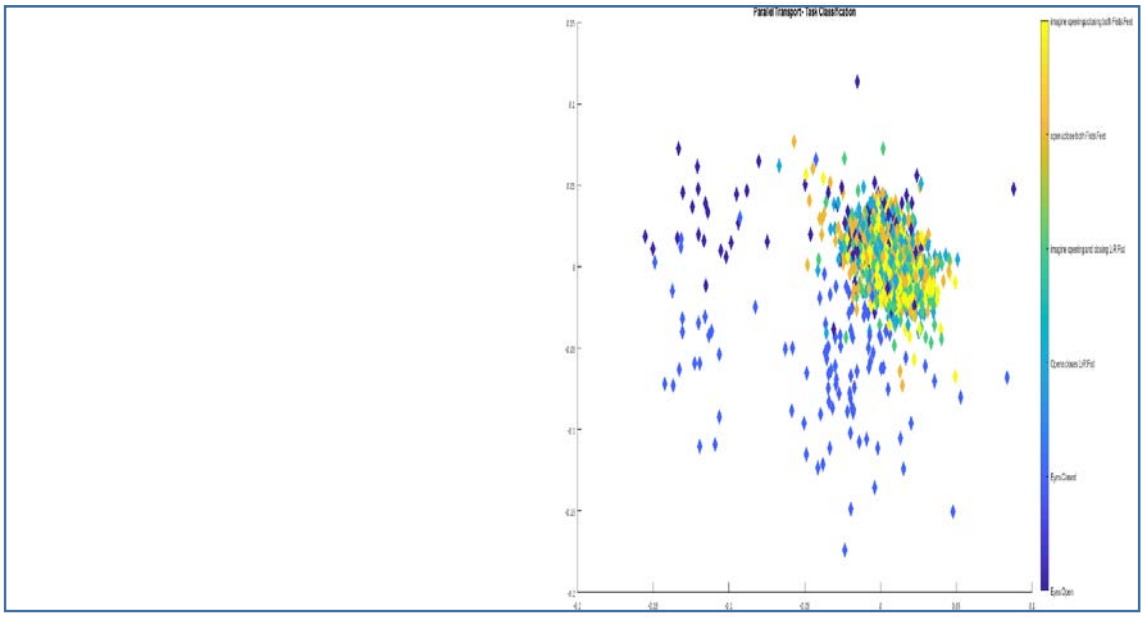

a b

Figure 1: Low dimensional representation for EEG signals. Left- before registration. Right- after PT.

(9)

Lung Segmentation from Chest X-ray Images for Use in Deep Learning Systems

Eliyahu Rosenfelder[1], Ilai Waimann[1], Amit Livneh[1], Yaron Blinder[2]

[1] Department of Biomedical Engineering, Technion - IIT, Haifa, Israel
[2] Radical AI

Introduction: Chest X-rays are the most common medical imaging exam today, comprising 40% of all medical imaging exams, and estimated at 2 billion exams per year worldwide. However, 50% of the global population have no access to radiology, and in the 1st world there is an average of only 10 radiologists per 100,000 patients. The average reported error rates of expert radiologists up to 10%-30%, and can be much higher in some reported cases where the diagnosis is given by unqualified doctors. For these reasons, many researchers and companies are developing machine learning & deep learning systems for automatic classification/diagnosis. A known issue with such algorithms is the need for large datasets, and the requirement for expensive computational power. Together with an industry partner, we hypothesized that using segmented lungs as input to a deep learning classifier would allow it to learn faster and better classify lung anomalies. The specific goal of our project was to develop and implement an algorithm to perform accurate segmentation of the lungs in chest X-ray images. The algorithm takes an Anterior-Posterior (AP) chest X-ray image as input, and produces an output image containing only the lung area. This is of great importance due to the extreme global shortage of radiologists and the high error rate of expert radiologist's diagnosis throughout the world.

Methods: Using a public dataset for testing and training, we implemented a series of functions using the python programming language and several open-source packages, including the OpenCV package (Open Source Computer Vision library), and SKlearn's Kmeans algorithm.

We used the Jaccard index, given by $J = \frac{TP}{TP+FP+FN}$ to quantify our algorithm's performance. Another measure of the performance is given by the accuracy: $Accuracy = \frac{TP+TN}{TP+TN+FP+FN}$.

Results: We report a Jaccard index of J = 79.87%, with an accuracy rate of 88.76%. The segments isolated by our algorithm reduce the image size by 55.62%, essentially doubling the signal to noise ratio. The segmented images produced with our algorithm are currently being used to train a large-scale neural network which will be combined with other classifiers trained on the entire images.

Conclusions: We have developed and implemented a lung segmentation algorithm for chest X-ray images to be used as a preprocessing tool for machine-learning based medical image classification tools. This tool is expected to enhance the specificity of such AI-based diagnostics, but further work needs to be done to fully integrate it into the AI training workflow.

Keywords: X-rays, segmentation, lung, machine learning.

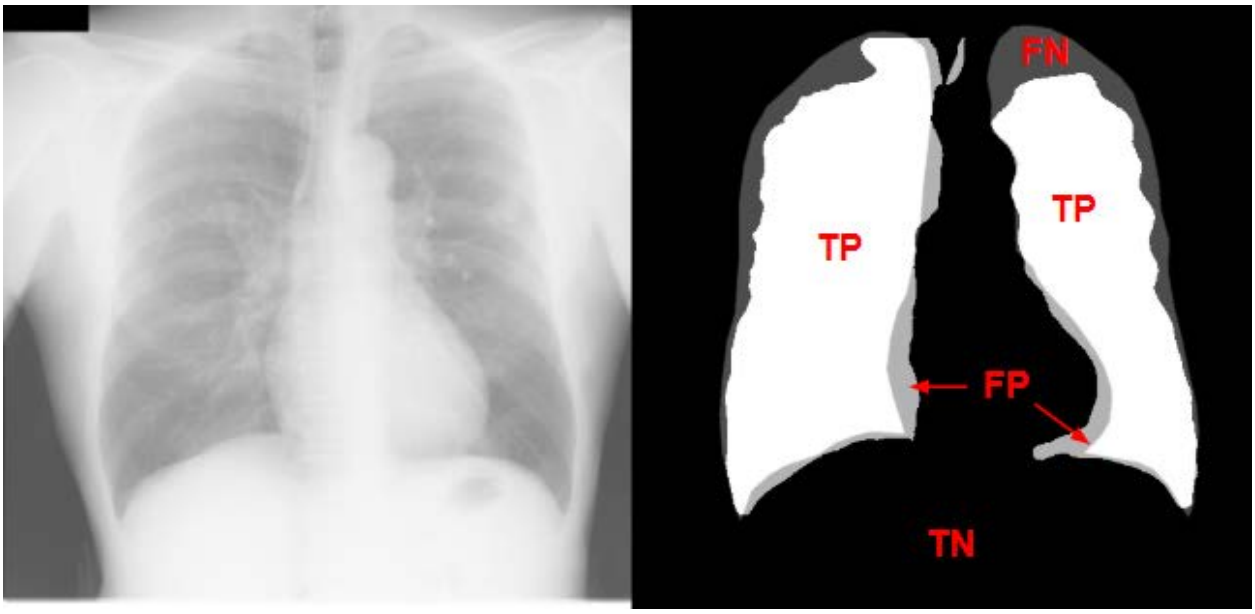

Figure 1: Example of comparing the segmentation of the lungs of our algorithm with that of expert radiologists, Chest X-ray from JSRT database. In this case J = 76%. T=True, F=False, P=Positive, N=Negative.

(10)

Non-Invasive Monitoring of Heart Failure Patients Using Respiratory Signals

Tomer Heitner[1], Noa Markovitch[1], Amit Livneh[1], Shmuel Rispler[2], Amir Landesberg[1]

[1] Department of Biomedical Engineering, Technion - IIT, Haifa, Israel
[2] Rambam Healthcare Campus, Cardiology Department, Haifa, Israel

Introduction: Heart Failure (HF) is an aggravating worldwide epidemic, affecting tens of millions. Patients affected are frequently hospitalized with dyspnea and fatigue, which greatly impair their quality of life. The frequent hospitalizations also present a considerable economic burden on the medical system. In the US, rehospitalization within 30 days (for the same reason) does not grant reimbursement. In medical literature, HF related pathologies are known to increase patients' respiratory effort, which ultimately leads to dyspnea. Currently, assessment and treatment are based on hemodynamic measurements, which do not evaluate the patients' respiratory effort. Patients are then discharged based on hemodynamic improvement, and are commonly readmitted shortly after, once again, with dyspnea. Herein, we study a method for objectively quantifying respiratory effort and dyspnea, in an effort to improve to patients' quality of life, and reduce their frequent rehospitalizations.

Methods: The study was approved by the Helsinki committee. Thirty-one decompensated HF patients (NYHA class 3,4), were recruited to the study upon hospital admission with dyspnea. To evaluate hospitalization benefit, respiratory signal acquisition was performed twice, first upon admission then preceding discharge. The patients were then followed until the next hospitalization due to dyspnea. Respiration was monitored by recording signals from miniature accelerometers attached to patient chest and epigastrium. The signals were analyzed in the time and frequency domain by a proprietary Matlab software, in order to calculate new physiologically inspired indices that quantify the patients' respiratory effort. In order to validate the new indices, the patients were assigned into two groups – (1) early-rehospitalization, within less than 30 days, (2) Late–rehospitalization, after more than 30 days. The indices were then tested for their ability to retrospectively predict early rehospitalization.

Results: Although the patients' condition and signals were considerably variable and challenging for computational analysis, some key distinctions between the groups of patients were made (Figure1). As the patient struggles to breath, excessive respiratory muscles are used to his aid, which can be seen in the signal in various ways (Figure1a): (1) Additional motion of the torso besides the regular motion in respiration – was detected as increased frequency content in the frequency analysis. (2) Forceful

expirations were detected as a great decent beneath a computer calculated, respiration rest amplitude – by extracting an index from this feature, we were able to predict late rehospitalization of patients with 75% sensitivity, and 11% FPR (Figure1b). Lastly, we noticed some of the early-rehospitalization patients had a unique breathing pattern with long apnea periods – known to indicate poor prognosis.

Conclusions: Our study demonstrated the feasibility to quantify the severity of HF patients' condition through computational signal analysis. We noticed that excessive respiratory effort, exerted by decompensated HF patients, alters the patient breathing pattern. These pathological changes can be analyzed and quantified, and new physiologically based indices can be extracted from them. With the new indices we can turn symptoms, namely dyspnea, into signs, predict and prevent rehospitalization, optimize treatment, and improve our patients' quality of life.

Keywords: Heart failure, Respiratory monitoring, Predicting rehospitalization

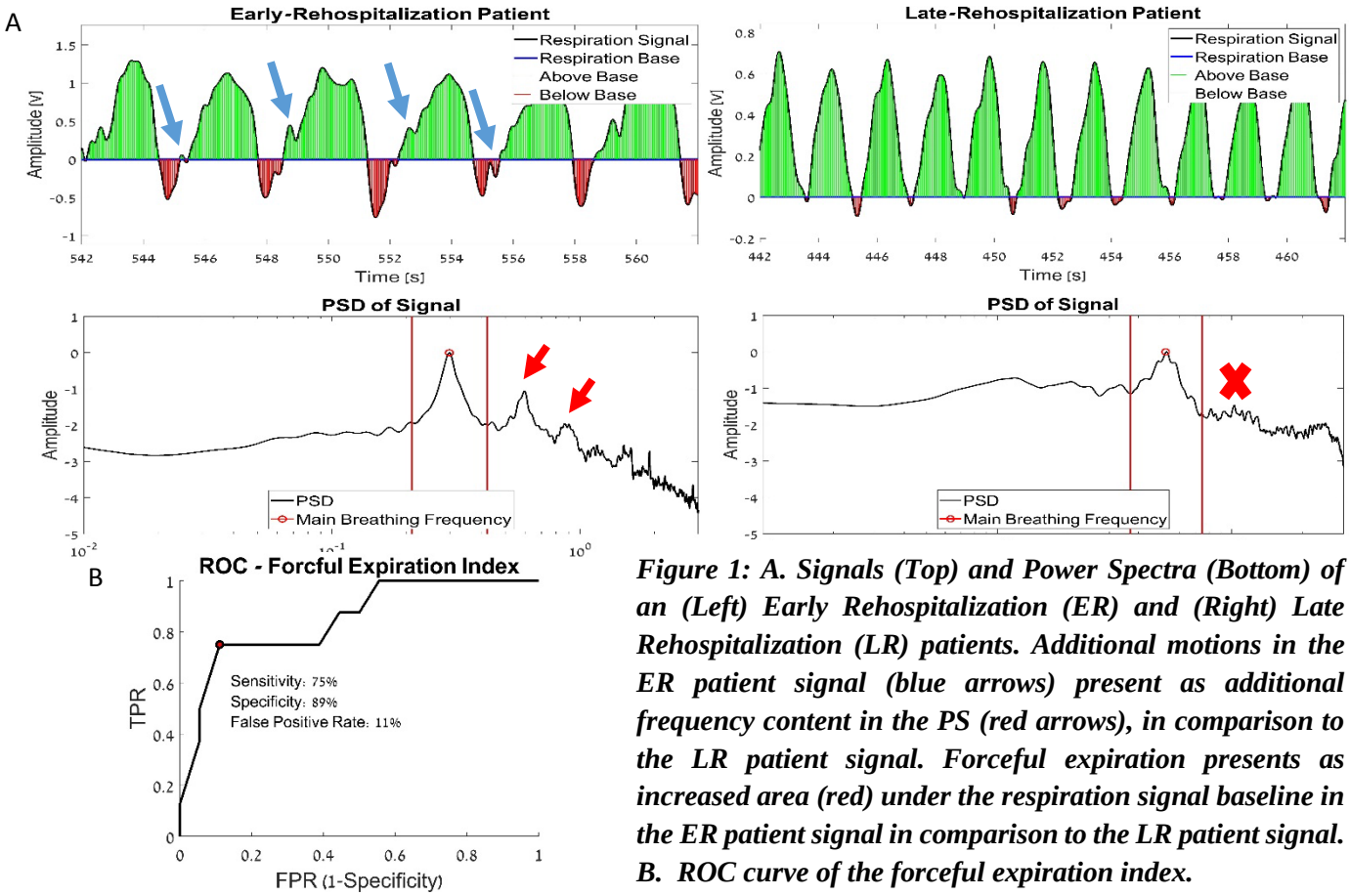

Figure 1: A. Signals (Top) and Power Spectra (Bottom) of an (Left) Early Rehospitalization (ER) and (Right) Late Rehospitalization (LR) patients. Additional motions in the ER patient signal (blue arrows) present as additional frequency content in the PS (red arrows), in comparison to the LR patient signal. Forceful expiration presents as increased area (red) under the respiration signal baseline in the ER patient signal in comparison to the LR patient signal. B. ROC curve of the forceful expiration index.

(11)

Focusing Quality in Transcranial MRgFUS by Shifting Phases from Reference Points

Ariel Veler[1], Eyal Abend[1], Oscar Lichtenstein[1], Yoav Levy[2]

[1] Department of Biomedical Engineering, Technion - IIT, Haifa, Israel
[2] INSIGHTEC Ltd, Haifa, Israel

Introduction: Insightech Ltd. is performing neurosurgery by Magnetic Resonance-guided Focused Ultrasound (MRgFUS), using multiple-element transducers. Accurate phase corrections must be applied to compensate the aberration generated by the skull and get a sharp focus. The estimation of the required compensations is currently made by previously scanning patient's head using computed tomography (CT) and applying physical and computational models. Under the assumption that recent undisclosed developments allow to accurately estimate the phase corrections from of a few specific reference points inside the brain, an alternative or additional technique is proposed and tested for focusing at some different positions than those of the reference points.

Methods: An ex-vivo experiment was performed using ExAblate-Neuro equipment. A previously CT-scanned human skull was placed in the transducer and filled with circulating water at controlled temperature. A hydrophone held by a set of controlled, motorized arms was inserted into the skull cavity and its relative position was set in several points in a volume of 17[cm^3] around the center of the transducer. For every target point, sonication at 650[KHz] of each one of the elements was executed separately with zero-phase, and the pressure waves were respectively measured in order to calculate phase shifts. Every two points were then considered as a pair of reference and target. Two models were proposed to estimate the phase correction at the target: (1) the measured phases at the reference plus shifting phases from one point to the other based on the difference between the phase estimates at both points as if there was no skull; and (2), adding also the difference between the CT-based phase estimates for the aberration in the skull for the two points. The focusing quality scores were computed by comparing the measured phases and the estimate ones for all the methods.

Results: For the current method of compensation, the maximal scores were obtained at the center of the transducer with an average of 75% in this experiment. For the new, a high dependency on the distance between target and reference was observed. There were not found statistically significant differences between results of method (1) and (2) in the general case. For both, the maximal focusing quality were obtained for the minimal distances between target and reference (2.5[mm]), with an average of 95%. For distances below 15[mm] it was found that the proposed methods improve with highly significance ($p < 0.0001$) the focusing quality compared to the current method.

Conclusions: The results suggest that given the eventual capability to accurately estimate phase shifts for some given points near the target of ablation in neurosurgical patients, high focusing quality can be achieved by using the presented methods.

Keywords: Magnetic Resonance-guided Focused Ultrasound Surgery, Skull aberration correction, Transcranial focusing, CT based focusing

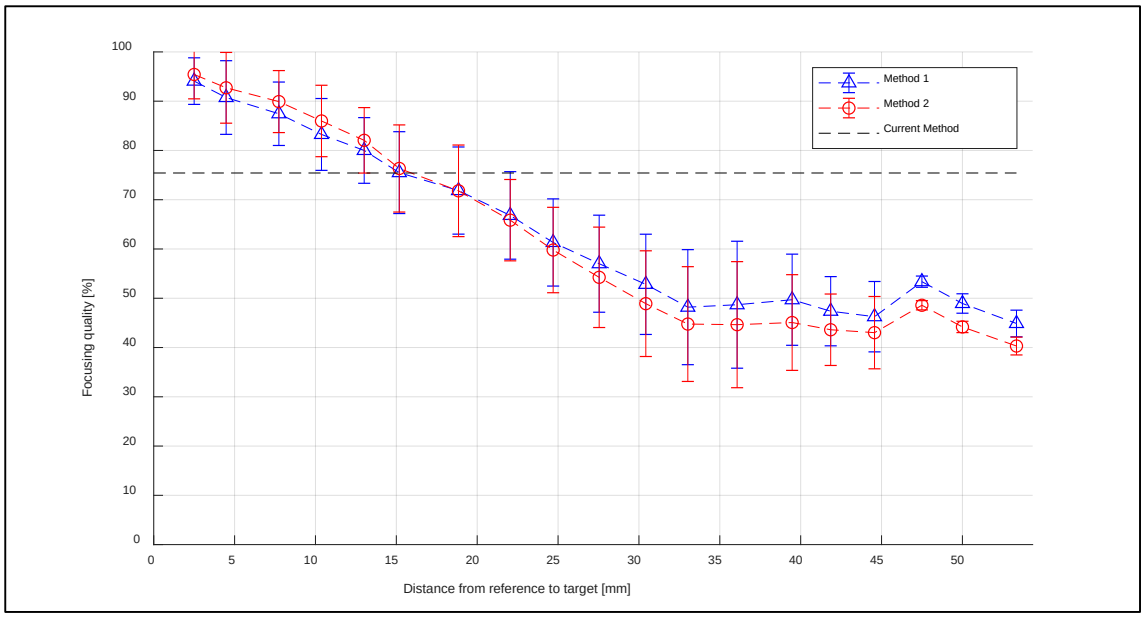

Figure 1: Focusing quality as function of distance between reference and target points

(12)

Predictive Model for the Onset of Atrial Fibrillation Events

Yonatan Elul[1], Assaf Shuster[2], Oscar Lichtenstein [1], Alex Bronstein[2], Yael Yaniv[1]

[1] Biomedical Engineering Faculty, Technion - IIT, Haifa, Israel
[2] Computer Science Faculty, Technion - IIT, Haifa, Israel

Introduction: Atrial fibrillation (AF), the most common sustained arrhythmia in the Western world, affects more than 6 million Americans, with a projected 10–14 million cases by 2030. Due to its association with increased risk for stroke, heart failure, and mortality, AF has a profound impact on patient longevity and quality of life. Current treatments are not only ineffective but may also decrease patient lifespan. Moreover, these treatments are administered only after AF induction. Recent studies suggest that atrial pacing, induced prior to an AF event, can successfully prevent re-initiation. However, no predictive system (or even a system that correctly identifies AF) exists.

Methods: We designed two models: the first is based on an original deep learning model inspired by Temporal Convolutional Networks and Convolutional Networks (TCNCN), and the second, based on a spectral clustering algorithm (SCE), employs a single novel index to quantify heart rate variability entropy distribution (SE) and distinguish two main groups of AF patients (each defined by a different intrinsic mechanism). Our SCE model uses an affinity metric, applied in the clustering process:

$$Affinity = e^{-|SE1-SE2|} \quad (1)$$

For the AF detection task, several TCNCN models were trained on long ECG recordings (~ 12h) of AF patients (n = 18) and then validated on separate ECG recordings (n = 2) in order to choose the best model. After the parameters for the best model were found, it was tested on similar ECG recordings of AF patients (n = 3) and healthy subjects (n = 3).

For the AF prediction task, we first used the SCE model to separate the ECG records into 3 groups: healthy subjects (H), AF patients from the first group (AFM1), and AF patients from the second group (AFM2). We then optimized the SCE model parameters for each group, creating 3 SCE models. These were evaluated on long ECG recordings (~ 24h) of AF patients (n = 84) and healthy subjects (n = 18). All ECG recordings are from Physionet.

Results: For AF detection, the best TCNCN model received a specificity score of 96.6%, and a sensitivity score of 18.3%.

For AF prediction, the three SCE models' scores are summarized in Table 1:

Group	Sensitivity	Specificity
1	26.6%	36.8%
2	58.3%	51.2%
3	100%	100%

Conclusions: The SCE model predicted AF onset perfectly for group 3, (n = 35, 34 w/ AF, 1 healthy), and with mediocre specificity for group 2. The TCNCN model very accurately detected AF events. We believe that training the TCNCN model on records from healthy subjects will greatly increase its specificity score. Those results indicate the way forward for future work, highlighting the improvements required for clinical-level accuracy, which could allow novel treatments for AF. We have also shown the possible existence of two underlying physiological mechanisms capable of inducing AF, and a machine learning algorithm to distinguish between them.

Keywords: Atrial Fibrillation; Deep Learning; Temporal Convolution Networks; Spectral Clustering.

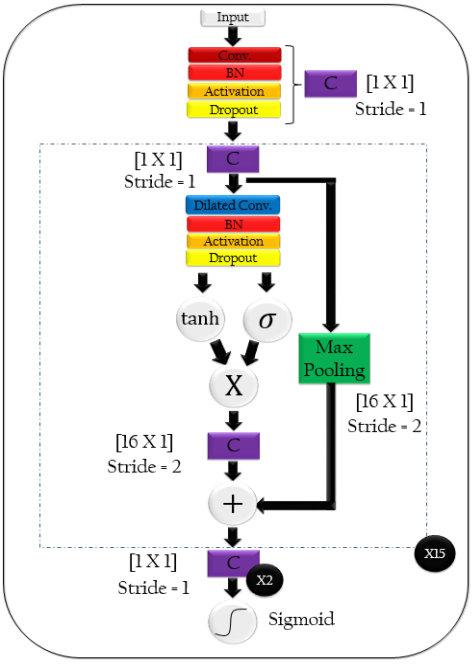

Figure 1: The TCNCN model architecture.
Conv. – Convolutional layer.
BN – Batch Normalization layer.
Activation – 'ReLU' layer.
Dropout – Dropout layer.
Max Pooling – A Max Pooling Layer.
σ (sigmoid), tanh – activation functions.
Sigmoid – Sigmoidal output layer.

(13)

Prediction of Ventricular Fibrillation Using Heart Rate Variability Indices and Artificial Neural Networks

Noam Keidar[1,4], Gal Eidelsztein[1,4], Ido Weiser-Bitoun[1], Shmuel Rispler[2], Assaf Schuster[3], Alex Bronstein[3], Oscar Lichtenstein[1], Yael Yaniv[1]

[1] Faculty of Biomedical Engineering, Technion IIT
[2] Heart Failure Unit, Department of Cardiology, Rambam Health Care Campus
[3] Computer Science Department, Technion IIT
[4] Faculty of Medicine, Technion IIT

Introduction: Ventricular Fibrillation (VF) is a lethal arrhythmia of the heart. VF is an important pathophysiological mechanism and it is the cause for cardiac arrest in the vast majority of sudden cardiac death events. Survival rates among victims can be as high as 90% in patients that are treated immediately, and they decay linearly by 10% for every minute of delay in treatment. Early prediction of VF events may shorten the delay in treatment, improve survival rates and clinical outcome and may be used as a window for preventive treatment.

Methods: Long (~24h) ECG recordings from VF patients (n=20) and from healthy individuals (n=17) from PhysioNet databases were analyzed using a state-of-the art R peak detection algorithm to extract inter beat intervals (RR intervals). For each time step in the RR interval time series, 120 last RR intervals were used to calculate a vector of 19 indices that quantify the variability of heart rate during the recent past. A causal temporal convolutional artificial neural network (TCN) was used to assess the risk of a VF event in the near future based on the present heart rate variability (HRV) vector and a few hours history embodied in some thousands of previous HRV vectors. Training of the TCN was done using Leave One Out testing.

Results: Nearly all alarms occurred in the VF patient population (PPV=?), however, no alarms were triggered in healthy individuals. On average, sensitivity and specificity were 62.5% and 100% respectively, Positive Predictive Value was 100%.

Conclusions: Prediction of fatal cardiac arrhythmias, hours to minutes in advance, may be possible. Model training using a larger cohort of patients should improve prediction performance and allow the utilization of arrhythmia prediction systems in medicine, potentially improving survival rates and clinical outcomes. Furthermore, the possibility to predict the onset of cardiac arrhythmias may also give insight into the pathophysiological mechanism of arrhythmia.

Keywords: Arrhythmia; temporal convolutional networks; heart rate variability; sudden cardiac death.

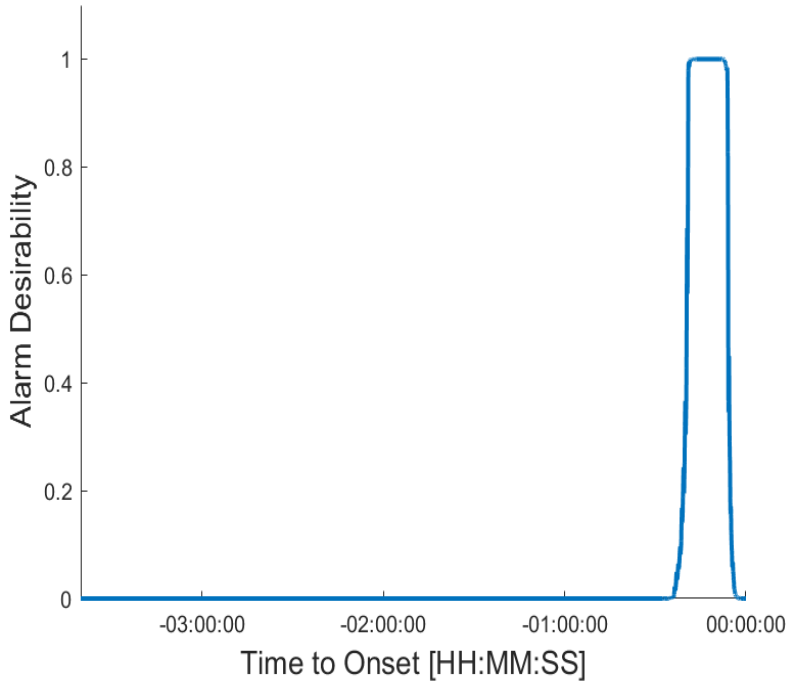

Figure 1: Prediction curve for patient #46. Threshold for alarm is 0.5, note that the alarm first starts 19 minutes and 38 seconds before onset of event.

(14)

Quantification of the Pulmonary Impedance and the Right Ventricle Contractility

Alon Sideman[1], Efrat Ben-Sadeh[1], Anna Faingersh[1], and Amir Landsberg[1]

[1] Department of Biomedical Engineering, Technion - IIT, Haifa, Israel

Introduction: Right heart failure (RHF) is usually an ominous outcome of left heart failure (LHF) or pulmonary diseases. Currently, the right-ventricle (RV) function and its interaction with the pulmonary system are not well quantified. A novel concept, denoted as the "work pressure time integral relationship" (WPTiR) was introduced and studied in Landesberg's lab, to quantify the interplay between the ventricle function and the loading conditions. The WPTiR depicts the ventricle external work (EW) against the pressure-time integral (PTi), which is a surrogate to the total energy consumed. It was shown that the WPTiR can identify the transition point of the cardiac adaptive response to decompensation, in a rat model of volume-overload induced heart failure. For the first time, this study applies the WPTiR concept for assessing RV function, in humans.

Methods: The study was approved by Rambam Helsinki committee, and was conducted in patients that underwent right cardiac catheterization for diagnosis of dyspnea and optimization of treatment. Time dependent pressure readings of the right atrium, RV, pulmonary artery (PA) and the pulmonary-capillary wedge, along with stroke volume measurements, were obtained from consenting adult patients (n=21). RV efficacy was assessed using the novel WPTiR index, by calculating the external work and the pressure-time integral. The PA dynamic resistance was quantified from the entire PA pressure dynamics, including both the systolic and diastolic phases.

Results: The study enrolled 21 patients that were classified into four groups: primary pulmonary arterial hypertension (PAH, n=4), interstitial lung disease (PPH, n=4), left heart failure (LHF, n=6) and left with right heart failure (RLHF, n=5). The other 2 patients couldn't be classified due to lack of information. Figure 1A depicts all patients in the WPTiR plane. The blue straight line presents the normal response to changes in the preload. Intriguingly, all patients are below this line, and present a larger increase in the PTI than in the EW, i.e. lower efficacy. The patients present a significant increase (155.91±73.14%) in the EW, thus cardio-pulmonary diseases are associated with a significant increase in the demand. The average cardiac index (CI) was 2.21±0.48 [$L{\cdot}m^2/min$]. The region below EW of 17% was populated with severely decompensated patients, with cardiac index (CI) of 1.86±0.22 [$L{\cdot}m^2/min$] (2.0 [$L{\cdot}m^2/min$] is the threshold for considering cardiac assist device). The energy consumption increases as the distance from the origin increases. Figure 1B presents the PTI against the pulmonary vascular resistance (R). All the patients fall within a well-defined region. The PAH and LHF groups exhibited a high mean PA resistance, of 7.59±1.81 and 6.69±2.31 [wood]. The

increase in the R is associated with a large increase in the PTI and larger energy losses (as heat).

Conclusions: The WPTiR plane is a useful tool for assessing RV performance, in humans. The utility in monitoring the progression of the disease and in optimization of treatment should be further investigated.

Keywords: Cardiac contractility, Cardiac mechanics, Ventricular-arterial coupling, Right ventrical failure, Heart Failure.

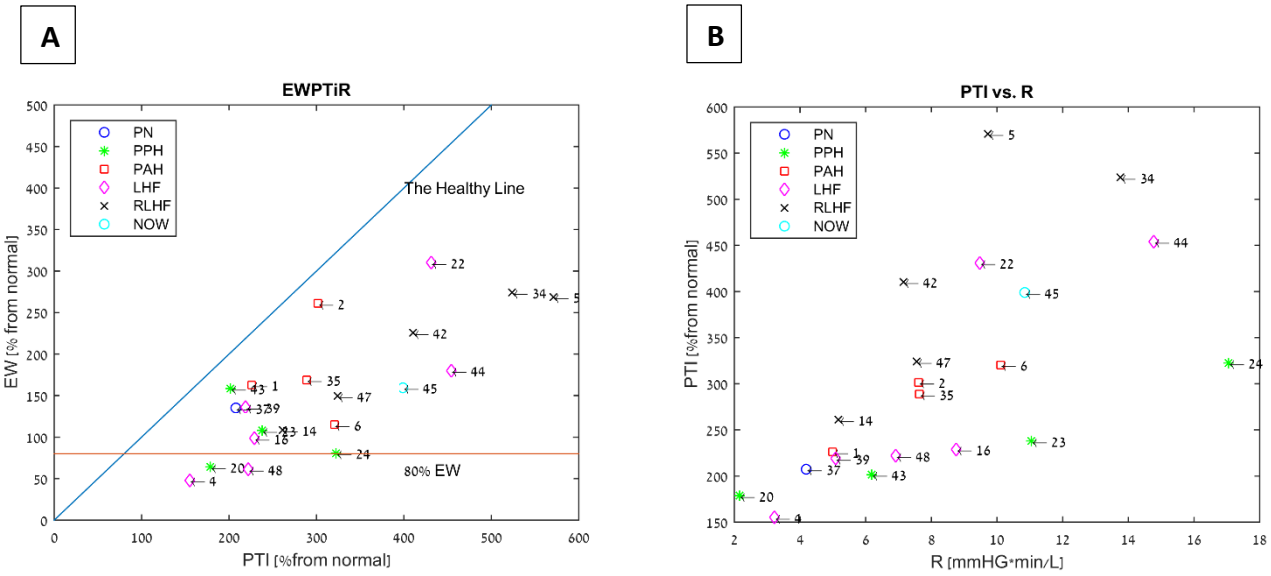

Figure 1: A, The right ventricle external work (EW) against the pressure time integral (PTi). B, The right ventricle PTI against the pulmonary vascular resistance.

(15)

Mass Deposition in Cerebral Side Aneurysms

Hadeel Ayoub[1], Mira Vintilescu[1], Mark Epshtein[1], Oscar Lichtenstein[1], Netanel Korin[1]

[1] Department of Biomedical Engineering, Technion - IIT, Haifa, Israel

Introduction: Thousands of deaths each year are caused by brain aneurysms with half the victims younger than 50-years-old. Available treatment is exclusively invasive. While non-invasive techniques are based on mass transport and deposition, current theories of mass deposition fail to accurately describe the observed experimental patterns. Better understanding of aneurysm mass deposition and more accurate mathematical models can be a guide to the design of efficient non-invasive therapeutic agents. Current theories describe particle deposition as function of wall shear stress (WSS), but it is not applicable in ultra-low WSS areas which are prevalent in cerebral side aneurysms. Here we propose an extension to the current WSS based theories which allows a more accurate prediction of mass deposition in some idealized cerebral side aneurysm models.

Methods: We developed a mathematical model to predict deposition rates in ultra-low shear regions and conducted computational fluid dynamics (CFD) simulations on three representative aneurysm geometries to demonstrate the predictions of both the current theory and our model. In addition, we conducted in vitro experiments on the same geometries, and compared the results of both methods.

Results: Our results show that contrary to current theories most of the particles deposited in ultra-low shear regions which our model predicts more accurately and closely resembles the experimental results.

Conclusions: The current mathematical model does not fully describe the experimental results and needs to be supplemented by a model similar to ours. However, more experimental work needs to be done to fully determine the unknown coefficients of our model.

Keywords: Mass deposition, Cerebral aneurysms, Targeted drug delivery

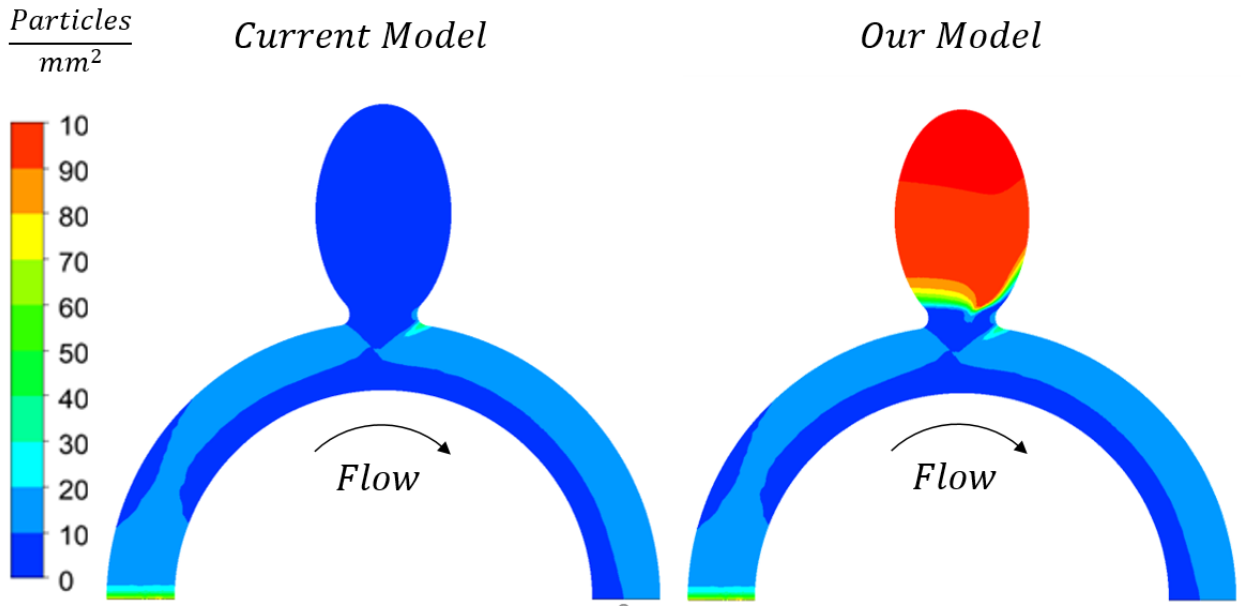

Figure 2: Mapping of particle deposition in one of the respresentative aneurysm geometries according to the current mathematical model (left) and our model (right). Inside the aneurysm where the WSS is ultra low, our model more closely resembles the experimental results. Outside the aneurysm for higher values of WSS, our model supplements the current one.

(16)

User Interface Design for a Low-Cost 3D Printed Electro-Mechanical Prosthetic Hand

Shunit Polinsky[1], Yair Herbast[2], Yoav Medan[3]

[1] Department of Biomedical Engineering, Technion - IIT, Haifa, Israel
[2] Department of Mechanical Engineering, Technion - IIT, Haifa, Israel
[3] Haifa3D Founder and Chairman, Visiting Scientist, Technion - IIT, Haifa, Israel

Introduction: The loss of one's hand can lead to a drastic reduction in the quality of life by decreasing the level of independence and the capability of performing activities of daily living. Various designs of prosthetic hands are available in the market, categorized as a mechanical, electrical and Myo-electric hand. Most of the advanced prosthetic hand available in the market based their design on an electromyogram (EMG) signal from the user's stump. However, this method is not suitable for all amputation cases, such as amputees who suffer from phantom pain when using the residual limb or people who suffer from permanent loss of the muscular action due to lack of physical activity and hence do not have sufficient EMG signal. There is a need to develop a prosthetic electronic hand that resembles the movements of the real human hand, performs functions like opening and closing of fingers and wrist rotation using signals from the user that are not direct signal from the residual limb.

Methods: The project present in this paper, aims to design a prosthetic solution to overcome the limitations of the current commercial prosthetic hands. The main objective of the project presented here is to have a prosthetic hand design for specific transradial amputee user's needs that are not met by the current prosthetic solution on the market. The main design considerations include:

1. electronic control that does not require a muscular activity of the residual limb,
2. lightweight,
3. reliable and durable,
4. intuitive and easy to use,
5. rotatable,
6. variable grip force pattern,
7. low-cost.

The solution presented here is an electronic hand that can perform a variety of user-defined hand configurations and grips by actively control flexion and extension of four fingers and rotation of the wrist with two different levels of grip forces. The mechanical system design that controls the movement of the fingers and wrist consists of four fingers with four different tendon-driven mechanisms actuated by four different micro DC motors, passive thumb with two discrete positions using two magnets and wrist rotation driven by gears and a DC motor.

All five independent micro DC motors are driven by a microcontroller system which measures the motors' current and consists of four buttons that can be pressed by the user. The adaptive control mechanism allows autonomous grip adaptation to different objects' size and shape, with different torque levels.

Results: For successful implementation of the device, feedback from the prospective user and feedback from healthy subjects were collected. Based on the feedback, device enhancements were implemented, and new user-inputs designs are planned for future studies.

Conclusions: Overall, our results showed that the prosthetic hand design represents a sufficient solution for several of the unmet needs of the prospective user and has the potential to give rise to a better and more suitable solution than the current commercial prosthetic hands with only minor design enhancements.

Keywords: electric prosthetic hand, current control, grip force level.

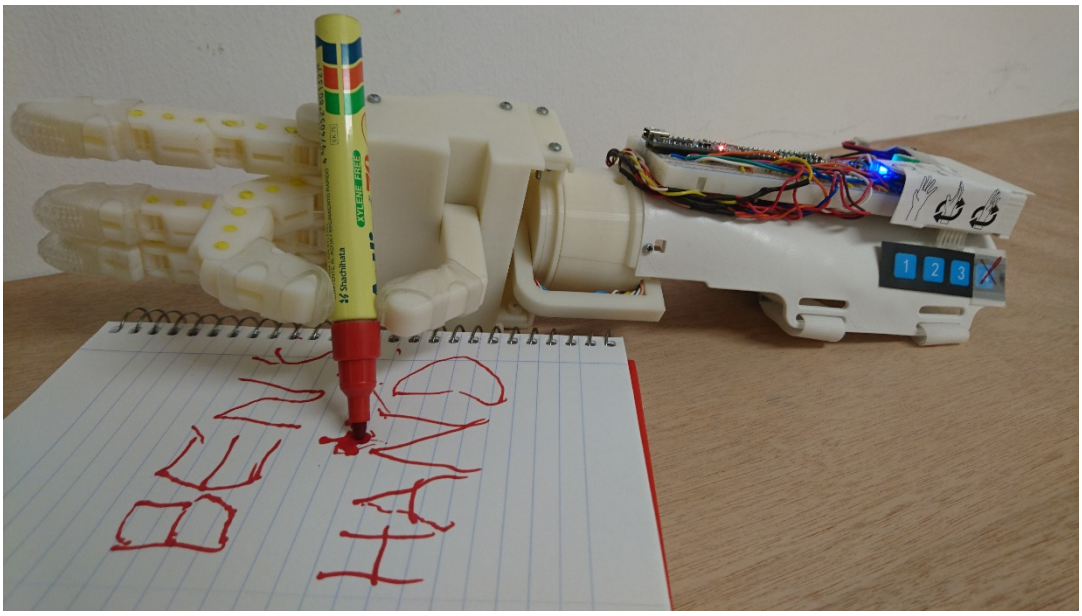

Figure 1: The electronic hand design. The device consists four buttons for user's input that send a signal to a microcontroller, which monitors the motors and buttons status and further transfers the command to actuate the motors according to the desired move.

(17)

Detecting DNA Mechanical Stretching under Flow

Ali Hilo[1], Rawaa Ayoub[1], Yathreb Asaad[1], Maria Khoury[1], Netanel Korin[1]

[1] Department of Biomedical Engineering, Technion – IIT, Haifa, Israel

Introduction: Von Willebrand factor (vWF), a plasma protein present in our circulatory system, plays an important role in primary hemostasis inside our bodies. vWF has a unique characteristic of changing its conformational state as a function of shear stress. Under these conditions, vWF changes its conformational state from globular to stretched thus exposing previously shielded domains. These domains interact with blood and extracellular components; mainly platelets and collagen. Inspired by its mechano-responsive exceptional behavior, vWF can be an interesting candidate for a targeted drug delivery carrier especially to high shear stress sites. As a preliminary step, we define a prototype for a similar mechano-sensitive biological moiety: DNA. DNA is also known to have a similar mechanical behavior as a function of shear stress. In this project, λ-DNA is chosen as a prototype that acts similarly to vWF. Our goal is to investigate the relationship between shear stress and the elongation of the λ-DNA. The main findings of this project will assist in better understanding of mechanistic insights of DNA and similar mechano-responsive moieties as vWF.

Methods: Our project aims at immobilizing λ-DNA via one end while the other is free floating. For so doing, we use avidin-biotin chemistry to immobilize the λ-DNA to the surface. At first, we biotinylate λ-DNA via one end by Klenow fragment enzyme, Biotin-dUTP, and a unique combination of other nucleotides. Then, we fluorescently label it with YOYO-1. The second part of the project is to build a microfluidic channel that enables us to expose the immobilized λ-DNA to different shear stresses. Convectional PDMS-based perfusion microchannel did not match our constrains therefore, we built a customized perfusion cell. As previously mentioned, for immobilizing the λ-DNA via one terminal, we use avidin-biotin chemistry. For this purpose, we need to functionalize the channel with low-density biotin and polyethylene glycol (PEG) to minimize the non-specific interactions with the surface. Finally, a syringe pump is used to set different fluid flow rates while confocal microscopy is used to visualize λ-DNA in real time.

Results: Our preliminary results suggest that, in the absence of flow and in low wall shear stresses, $\tau_w = 0 - 0.01\ dyn\ cm^{-2}$, the λ-DNA exhibits a compact and globular conformation. However, at higher flow rates, $\tau_w = 0.1 - 1\ dyn\ cm^{-2}$ λ-DNA elongates and its extension increases with increasing shear stress reaching maximum length of 11.82 μm. At higher flow rates, $\tau_w > 1\ dyn\ cm^{-2}$ no additional extension in length is observed.

Conclusions: We succeeded to design a perfusing chamber using functionalized coverslip and PDMS channel that manages us to expose the immobilized λ-DNA to different shear stresses, biotinylating and anchoring the λ-DNA via one end also minimizing non-specific interaction. However, several challenges have appeared. Our perfusion cell is based on glass slide as a mechanical supporter. This substantially reduces the imaging resolution. For better detection of the elongated λ-DNA, we need to use x60 oil objective with glass coverslip as a channel base. For this reason, we are trying to construct another version of a perfusion chamber that can enhance the resolution.

Keyword: λ-DNA, shear stress, Biotin-avidin

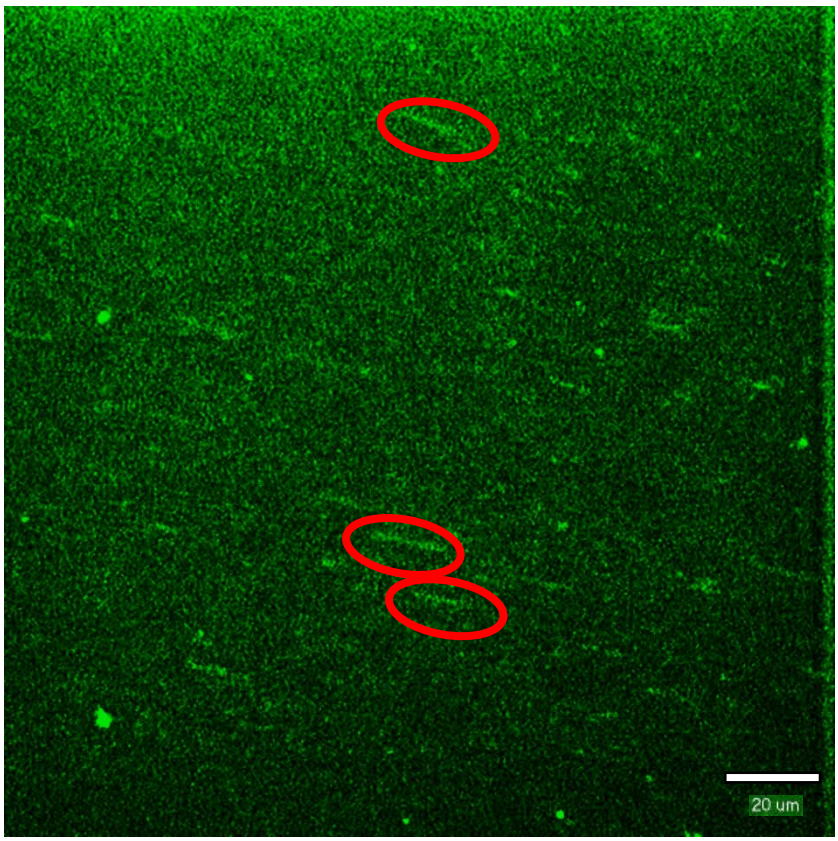

Figure 3: Immobilized λ -DNA via one end elongates under a shear stress of 1 dyne cm^{-2}

(18)

Low-Cost 3D Printing for Tissue Engineering

Dana Azagury[1], Moran Moradi[1], Ariel Szklanny[1], Maria Khoury[1], Shulamit Levenberg[1]

[1] Department of Biomedical Engineering, Technion – IIT, Haifa, Israel

Introduction: Tissue engineering is a rapidly growing multidisciplinary field, aimed at developing solutions for treating a variety of physiological ailments, including repairing sick or injured tissue, and replacing missing tissue. 3D printing is a layer-by-layer fabrication technique that is gaining wide attention, with applications ranging from metallurgic industry to biomedical applications. Bioprinting is the controlled deposition of biomaterials or cell aggregates in a controlled fashion, to achieve organized engineered tissues. Bioprinting presents many advantages, offering higher fabrication control, better distributed cell deposition and greater repeatability, when compared to more traditional techniques. Although, bioprinting represents a powerful technique, its cost is a critical drawback. Bioprinter prices range from $10.000, up to $250.000, depending on the printer's complexity and functionalities. These high prices can be a deterrent for small labs and hospitals to own and utilize 3D bioprinting.

Methods: We designed and printed poly-lactic acid (PLA) pieces, and transformed the original material deposition system of a Prusa i3 MK2 (Prusa, Checz Republic) printer into a syringe extrusion mechanism. We modified the extrusion stepper motor wiring to correct the extrusion direction. To support the new type of 3D printing, and avoid unnecessary printing movements, we studied and reprogrammed the automatically generated G-code, language that translates the model STL file into the printer's actions. As a next step, we calibrated the printer's extrusion rate and print speed, two key parameters controlling the resulting material deposition, aiming to print with a line width similar to the needle's inner diameter. Next, to improve the printer's capability of printing thick tissues, we recreated the 'Freeform Reversible Embedded of Suspended Hydrogels' technique, developed by Hinton *et al.* (Sciences Advances, 2015), consisting of printing hydrogels within a gelatin support material. We fabricathe slurry, and used a 4% alginate solution as bioink. Furthermore, to prove the printer's cell printing capability, we suspended dental pulp stem cells within the bioink, and printed a solid object, and performed live/dead assay. Lastly, we printed a bioreactor mold out of PLA, and then casted it with PDMS.

Results: In this work, we modified a filament-fusion 3D printer Prusa i3 M2K printer, achieving biomaterials and cells printing. We found that with an extrusion rate of 1 and a nozzle speed of 30 mm/sec we could achieve a ratio of 1.07 between the obtained printed band thickness, and the inner needle diameter (337 µm). We then printed vascular-like structures, with an inner diameter

of 3 mm. When printing cells suspended in the bioink, we obtained a cell viability over ~90%. Finally, our bioreactor allowed us to perfuse the vascular structure.

Conclusions: We managed to modify, for the first time to our knowledge, the Prusa i3 MK2 printer, allowing biomaterial and cell deposition. This printer can be purchased and modified for less than 1000$. Cell viability, using the modified printer, is comparable to the values of commercially available 3D printers. Lastly, our *ad hoc* bioreactor presents the advantages of being easy to make, requires cheap material, and is highly customizable to satisfy a wide range of applications.

Keywords: Bioprinting, Tissue Engineering, Flow bioreactor

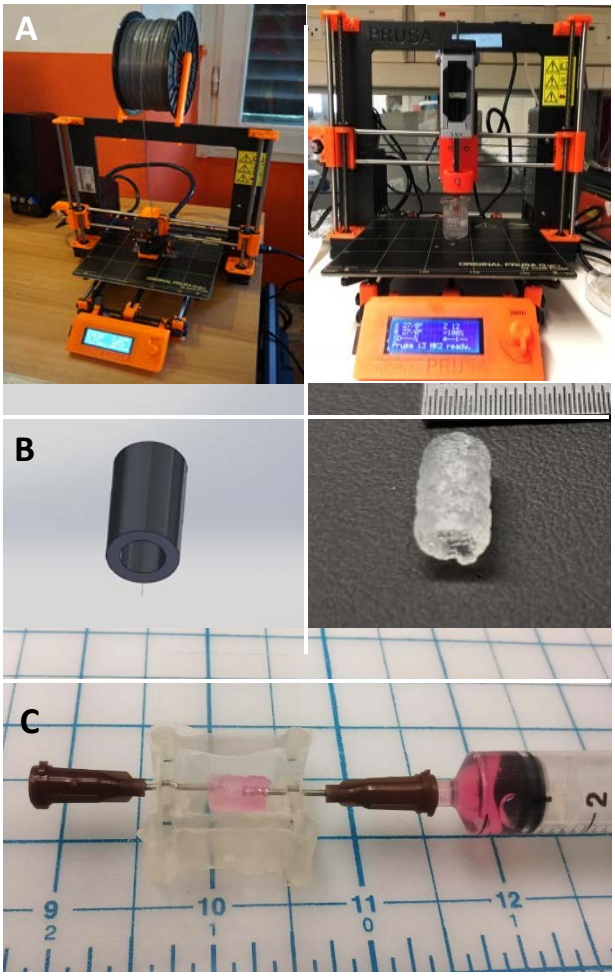

Figure 1: A: Left, Prusa i3 M2K without modifications; right, after the modifications for bioink deposition. B: Left, Solidworks model of vascular-like structure; right, alginate vascular-like structure printed within a gelatin support material. C: Perfused alginate scaffold within PDMS flow bioreactor.

Bio-fluids Lab

(19)

Investigation of Particles Deposition Using a 3D Bronchial Airway Model

Nofar Azulay[1], Eyal Habif[1], Shani Elias-Kirma[1], Maria Khoury[1], Josue Sznitman[1]

[1]Department of Biomedical Engineering, Technion – IIT, Haifa, Israel

Introduction: Exposure to inhaled particulate matter is a major risk factor that could lead to severe lung and heart diseases. Former research continue to support a link between urban air pollution and an increased incidence of airway diseases such as asthma and COPD.

Investigate the way in which particles deposit in the upper airway may provide an essential information toward tissue healing and damage assessment.

Methods:

1. 3D airway model simulating physiological upper airways
   We used a model that was designed according to a geometry parameters taken from former studies, in order to simulate 8-10 airway generations. The model was prepared from Polydimethylsiloxane (PDMS) and attached to a slide glass.
2. Aerosol Generator system
   We used aerosol generator device to generate aerosols from suspended 2 micrometer fluorescent Polystyrene particles in distilled water. The experimental system was built by connecting the aerosol generator to several models via bifurcation tubes. Using this system, we were able to control two parameters that may influence deposition pattern; a. placing the models in different directions to test gravity effect; b. changing flow rates to simulate heavy and quiet breathing conditions.
3. Image acquisition and data
   Images of the models were taken using a florescent microscope after 1 hour and 2 hours. Using image processing tools we divided the model into 7 segments and for each segment we calculated the amount of particles per area.

Results: We compered particles density (particles/mm^2) obtained from each generation. Results show an increase in particle density as generations grow as expected. In order to examine the effect flow rate has on deposition, two models were placed at the same orientation but under different

flow rates (i.e heavy and quiet breathing). Higher deposition density was obtained in quiet breathing compared to heavy breathing. Moreover, to investigate the gravitational settling effect, we compered two models that were under the same flow rate but placed in different gravity angle (defined by the angle between the vector which lies in the axis of the airway upon inspiration and the gravity vector). We observed that the model placed in a gravity angle of ~60° showed higher deposition density than the ~120° gravity angle.

Conclusions: We achieved a stable and reliable experiment system that simulate particle deposition through the upper airways. Utilizing the system for further research may improve the investigation of deposition properties, and subsequently help drug delivery and tissue repair research.

Keywords: Deposition, Air way model, Pollution

A B

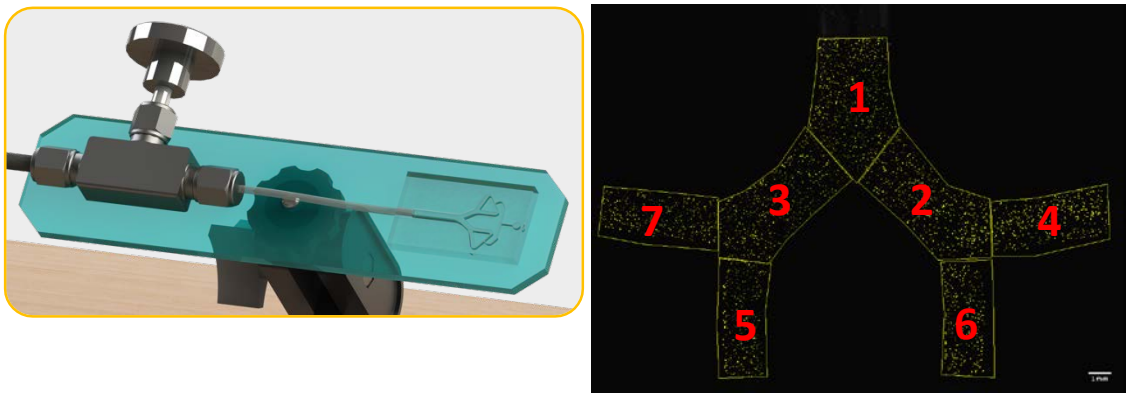

Figure 4: Illustration of the experiment system showing the aerosol generator connected do the 3D model while flow rate can be modified by valve (A).The output of the image obtained from the microscope, after applying image processing tools for segmentation and particle detection (B).

(20)

Utilizing 3D Printing for the Fabrication of Precision Scaffolds for Spinal Cord Injury Repair

Noah Michael[1], Tsemach Bar-Mucha[1], Idan Redenski[1], Ben Kaplan[1], and Shulamit Levenberg[1]

[1] Department of Biomedical Engineering, Technion - IIT, Haifa, Israel

Introduction: The inability of severed axons to regenerate in the spinal cord poses a constant challenge in the medical world due to local inflammation, inhibitory molecules, and lack of extracellular matrix. Synthetic scaffolds and gels have been used to address the loss of extracellular matrix. However, methods to mimic the architecture of the spinal cord are limited. Specifically, fabrication methods lack accuracy and control over the topographic cues of the scaffolds. Here we report a novel method to utilize 3D printing in order to introduce a controlled and accurate design into biocompatible and biodegradable scaffolds. In addition, we combined freeze-drying along with 3D printing to generate micro-pores which promoted nutrient diffusion, vascularization, and cell attachment to support regenerating axons.

Methods: We designed the optimal template using Solidworks, 3D Slicer, and custom G-code editing, then printed it on a step motor printer. We chose Butanediol vinyl alcohol (BVOH) as a water soluble, printable material. Using a bio-dynamic test instrument, we measured the Young's modulus of various materials to determine the optimal polymer in terms of similarity to spinal tissue and biodegradability, then casted that polymer into the template. Using a freeze-drying technique, we lyophilized the polymer within the template. Finally, we dissolved the template in water and were left with a transplant-ready scaffold.

Results: We found that a 5% PLLA/PLGA polymer best fit our requirements, as it was similar in softness to spinal cord tissue, yet stable, and suitably biodegradable. We designed a novel, effective template and scaffold, achieving optimal channel diameters of less than 250 micrometers and a vast network of interconnected micropores surrounding the channels. We reached high values of open volume and porosity in our scaffold, and witnessed remarkable vascularization and cell-growth following dental pulp stem cell seeding. In addition, we designed a complex template which could be easily altered to fit different spinal cords and specific injuries.

Conclusions: We found that 3D printing can be used to fabricate a scaffold with great precision and adaptability. The various elements of the process, such as the polymer used and both the micro and macro dimensions of the design can be easily and quickly changed to fit specific spines and injuries. In addition, the incorporation of a micropore network provides an excellent cellular environment, allowing for the growth of extracellular matrix and vascularization.

Keywords: Spinal-cord injury, 3D printing, Axonal regeneration, Tissue engineering

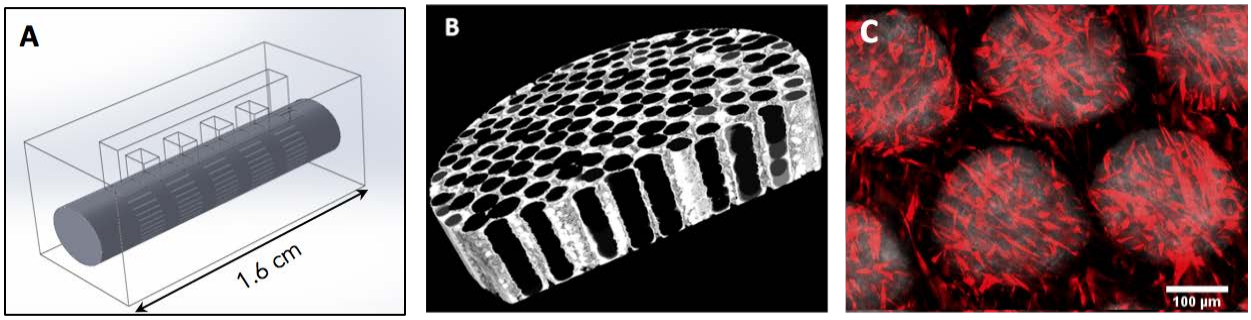

Figure 1: Design and characteristics of the scaffold. (A) The measurements and shape of a rat spinal cord are fitted with a unique microstructure as designed on SolidWorks. (B) A µ-CT scan of the fabricated scaffold, with clearly visible, numerous micro-channels. (C) Dental Pulp Stem Cells (DPSC) which secrete neurotrophic factors and support axonal regeneration, properly attach and grow inside the scaffold.

(21)

Double-Network Hydrogels for Cartilage Repair

Liaura Ifergan[1], Sapir Cohen[1], Haneen Simaan-Yameen[1], Tamara Birman[1], Olga Kossover[1], Dror Seliktar[1]

[1]Department of Biomedical Engineering, Technion – IIT, Haifa, Israel

Introduction: Joint-related injuries have been reported as one of the western world's most challenging health problems. The standard therapy strategy for minimal cartilage injury is cell implantation using a procedure called autologous chondrocyte implantation (ACI). In this procedure, a biopsy from a healthy cartilage region is taken, followed by cell culturing and re-implantation. ACI is currently performed by using a periosteum pouch to enclose a solution containing cells. However, this method is found to be ineffective, due to the immune system's negative reaction and cell solution leakage to the blood stream. Herein, we propose designing a unique hydrogel system that will provide optimal and favorable healing and will support mesenchymal stem cells (MSCs) viability, cell proliferation and cell differentiation into chondrocytes. We explored an innovative hydrogel combination of PEG-fibrinogen, with a guest-host hydrogel system based on hyaluronic acid (HA). PEG-fibrinogen is a covalently cross-linked biocompatible and biodegradable polymer that induces cell adhesion and encourages the replacement with autologous tissue. Due to dynamic interactions, the guest-host network provides shear-thinning and self-healing properties, generating an injectable material for minimally invasive implantation.

Methods: We analyzed different hydrogel combinations including PEG-fibrinogen, guest-host HA and PEG-DA monomers. To study the influence of viscosity on chondrocytes, formulations of guest-host HA were tested (2% and 5%). Increasing percentages of PEG-DA were added to those formulations to understand the influence of elasticity. We examined adaptability and viability by performing Live/Dead assay, using calcein/ethidium staining, on chondrocytes and on hMSCs under chondrogenesis conditions. Next, using dimethylmethylene blue (DMMB) assay, we quantified sulfated-glycosaminoglycan (GAGs) content to measure cell differentiation. All experiments were performed for 21 days.

Results: The more viscous formulations (5% guest-host) showed poor viability and generated a non-homogenous double-network hydrogel. The 2% guest-host formulations exhibited improved viability for both chondrocytes and hMSCs and, were thus chosen for following experiments. As seen in Fig.1, cells were more spread out and created an interconnected network respectively to the increasing PEG-DA content (0.2%, 0.5%, 1% and 2%). Cell differentiation process, indicated

by GAGs formation, was the highest for 0.5% PEG-DA addition.

Conclusion: The poor viability of 5% guest-host formulations is a result of the considerable mechanical stress that was applied on the cells during the viscous hydrogels preparation. Viability fluctuations observed in 2% guest-host formulations may originate from cell adaptation to the new matrix and differentiation process that alter both growth and death rates.
As mentioned above, the contrasting viability and GAGs assays results leads us to believe that a negative correlation exists between chondrogenesis and the unique morphology of the cells. It may be concluded that high values of viscosity stabilize cells adherence to the matrix and moderate chondrogenesis. Indeed, we suggest that the most suitable formulation is 2% guest-host HA 0.5% PEG-DA, which mimics the innate cells' environment and encourage differentiation. In order to validate this hypothesis, further immunostaining experiments will be performed.

Keywords: cartilage tissue engineering, cartilage injury, double-network hydrogel.

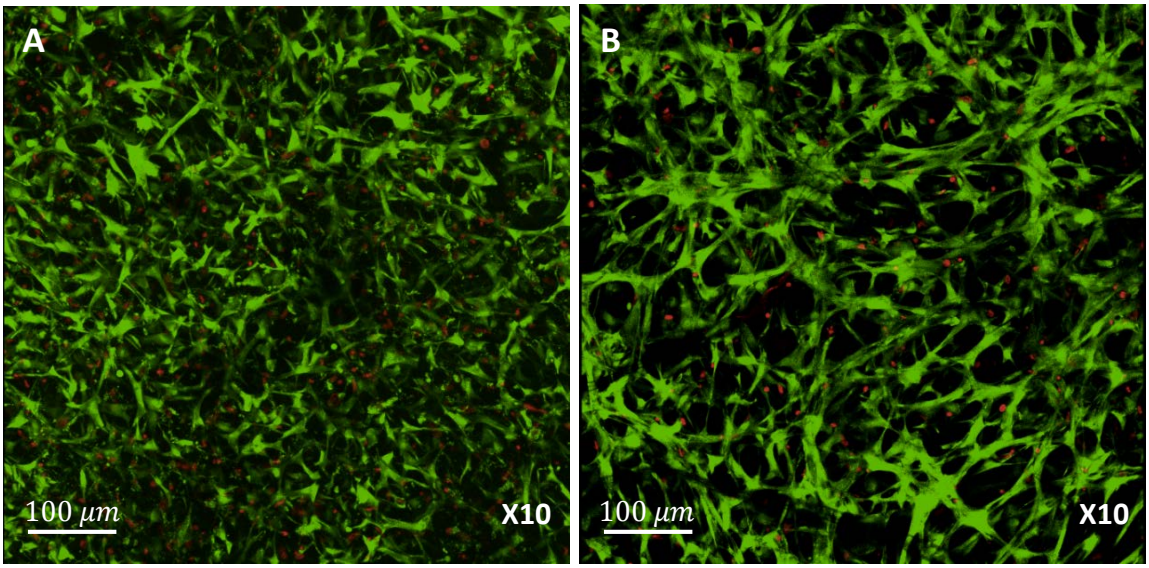

Figure 1: Viability of hMSCs in the double-network hydrogels. Live/dead staining with calcein (green) and ethidium (red) shows a relatively high number of viable cells within the hydrogels, when cultured for up to 21 days in chondrogenesis medium. (A) In 0.5% PEG-DA 2% gest-host HA formulation, more cells differentiated which created a less interconnected network, while (B) 2% PEG-DA 2% gest-host HA formulation induces the opposite

(22)

Nano-technology for Methylation Site Detection

Tal Elmalich[1], Chen Torfstein[1], Amit Meller[1]

[1] Department of Biomedical Engineering, Technion - IIT, Haifa, Israel

Introduction: Cancer is one of the largest concerns of our century. The disease mechanism has been broadly investigated over the years in order to develop better treatments and allow early detection. Aberrant DNA methylation patterns are crucial due to their role in gene expression regulation and due to the mounting evidence that they can lead to cancer development. In this research, we offer to utilize nano-pore technology and methyltransferases (MTases) to label the DNA with a bulky group of specific unmethylated sites to detect individual CpG sites in oncogenes and TSGs and develop a method for early detection of cancer based on detection of epigenetic changes.

Methods: Nanopores are e biosensing devices composed of a nanoscale pore, with dimensions around 2-10 nm that penetrates an insulating thin solid-state membrane (10-15 nm thick) with a constant electrical potential. The membrane separates two chambers, cis and trans, containing an electrolyte solution (buffered 1M KCl). When voltage is applied (300mV), a steady-state ionic current is generated. Charged molecules, such as DNA, are electrophoretically driven and hence translocate across the pore. Here, we label PCR amplified DNA using Taq1 Methyltrasferase, which transfer a bulky group called Gamma Cyclodextrin (γCD), to the Adenine residue in the recognition sequence (TCGA). The labeled DNA has a wider diameter than the bare DNA, and therefore when it passes through the pore, it blocks a higher percentage of the pore, resulting in a bigger drop in the ionic current. The current is recorded over time with the following parameters; I_o- open pore current, I_b- blocked pore current, t_D- duration of blockage. When DNA translocating through the pore the ratio $I_B = \frac{I_o}{I_b}$.

Results: By labeling 3532bp DNA which has only one M.Taq1 site and passing it through the pore we were able to have a proof of concept of our ability to label and detect γCD, using our nanopore setup, by observing two distinct levels of current blockage. Later we labelled a PCR amplified TSG, CDKN2B which serves as a biomarker in many cancers. This gene has 6 M.Taq1 sites, that are in a relatively close proximity, therefore, we could not obtain 7 different blockage levels as expected, but we did observe more than one.

Conclusions: Bulky group labelling is an exciting new approach for labelling CpG islands along the DNA. This method allows observing individual CpG sites, which is currently impossible using fluorescent labeling.

γCD may be used to label distanced CpG sites. To label closer sites there's a need of a different functional group. It is also important to understand the nano-pore technology is a very sensitive technique and hence the results may be influenced by miss-conducting any step in the process, or by very small molecules, such as dust, interfering with the system.

Keywords: CpG, Methylation, Nanopore, γCD/bulky group

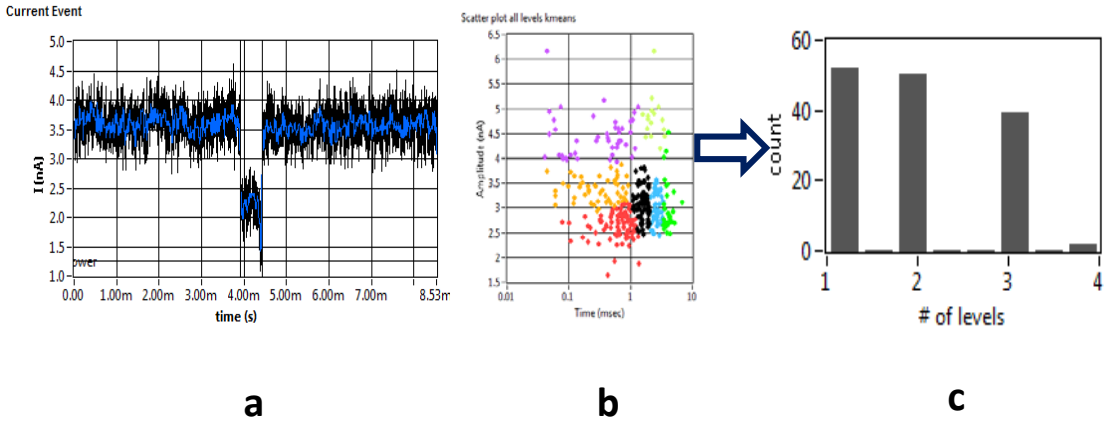

Figure 1: a- a singular event of CDKN2B strand of DNA translocating through the nanopore. B- scatter analysis: all events presented by the amplitude of blocked pore current as a function of duration of translocation. From b we can extract c- histogram describes the amounts of events and the number of levels they demonstrated.

(23)

3D Localization Microscopy by PSF Engineering in Live U2OS Cell Line

Maisa Nasser[1], Reem Shalaata[1], Tal Naor[1,2], Yoav Shechtman[1,2]

[1] Department of Biomedical Engineering, Technion - IIT, Haifa, Israel
[2] Lorry Lokey Interdisciplinary Center for Life Sciences and Engineering, Technion - IIT, Haifa, Israel

Introduction: Observing DNA inside cells has an increasing number of applications on chromatin structure and dynamics. Chromatin structure, organization, and dynamics play an important role in genome regulation. The majority of current knowledge about chromatin organization, has been obtained by chromosome structure capture (3C and related methods), which are methods that use high-throughput sequencing to provide evidence of proximal interaction between two loci which may be distal in genome sequence. Better understanding of chromatin dynamics is achieved by live cell imaging of DNA loci. Real-time observation of transcriptional processes or specific chromatin loci dynamics requires a combination of sequence-specific DNA labeling and precise 3D localization over time. Fast 3D localization with high spatiotemporal resolution is enabled by point spread function (PSF) engineering (creating a phase mask). Here we wished to demonstrate the potential of PSF engineering to enable precise 3D localization over time, by labeling specific (MUC4) and nonspecific (telomeres) DNA loci in live human bone osteosarcoma (U2OS) cells.

Methods: For labeling the specific locus two plasmids were used, first was the sgRNA coding plasmid targets repetitive locus in Muc4 gene using golden gate assembly, second was spdcas9-mcherry coding plasmid (gift from Thoru Pederson, Addgene plasmid # 64108). Then these two plasmids were co-transfected to U2OS cells, using Lipofectamine 3000 (invitrogene, Termo). For non-specific we used DsRed-TRF1 coding Plasmid and transfected it into U2OS cells for telomeres labeling.

Results: the images of labeled telomeres in live cells are shown in figure 1. As we can see by using PSF engineering more data from emitters that are not on focus was acquired (images a and b). The shape of the PSF codes the distance of the dot from focus, as shown in image c the right blue circle describes a PSF on the focal plane, while the left circle describes a PSF under or above Z plane.

Conclusions: PSF Engineering enables fast 3D localization of multiple particles over time in high spatiotemporal resolution, however in this case the emitter density was very high, and therefore, optimization of the PSF sensitivity is needed for improving the localization accuracy.

Keywords: DNA labeling, PSF engineering, Crisper dcas9 labeling.

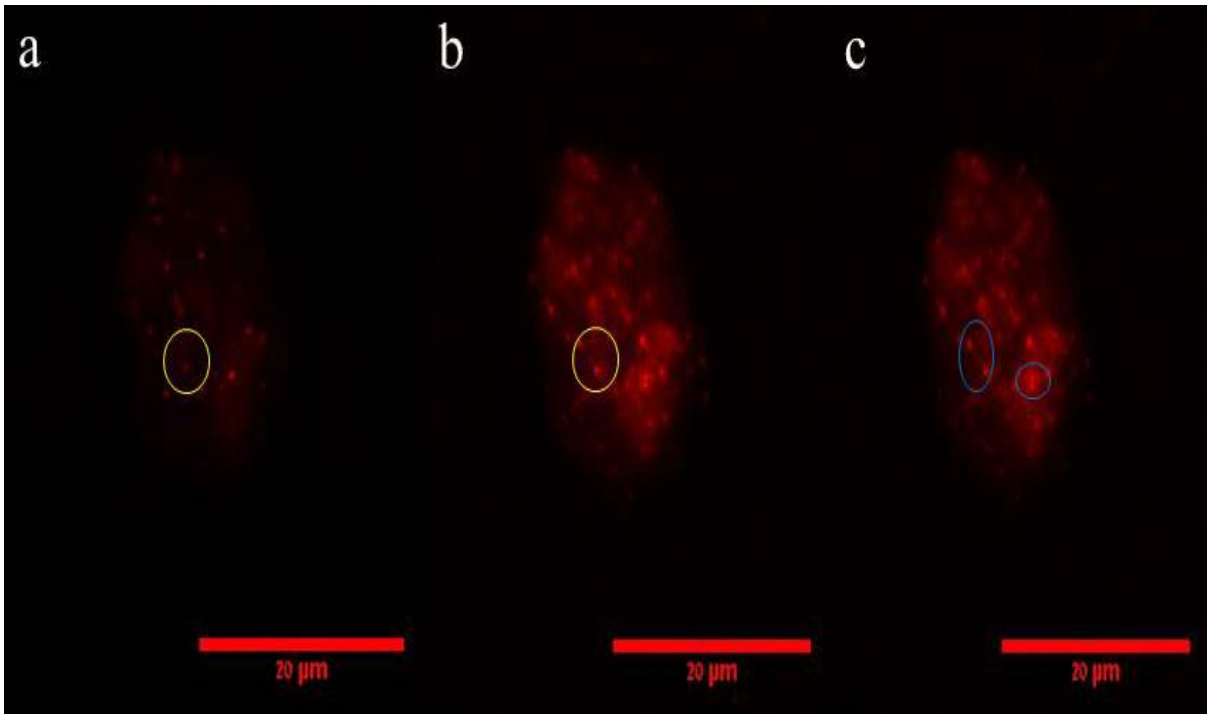

Figure 1: (a) Images of telomeres in live cell without phase mask, (b) Images of telomeres in live cell with phase mask (c)PSF in various z-positions.

שלום רב,

אנו שמחים להציג בפניכם את תקצירי הפרויקטים של הסטודנטים המסיימים לימודיהם בשנה זו, שנת תשע"ח.
הפרויקט, המבוצע ע"י סטודנטים בשנת הלימודים האחרונה, מהווה את גולת הכותרת של לימודיהם לתואר בהנדסה ביו-רפואית.
במסגרת הפרויקטים מביאים הסטודנטים לידי ביטוי את הידע והכלים שרכשו במהלך השנים בתחומי ההנדסה, המדע והרפואה.
מטרת הפרויקטים הינה לתת מענה לצרכי הפיתוח והמחקר של חברות העוסקות בתחום ההנדסה הביו-רפואית, תוך עמידה בסטנדרטים המקובלים ובמקביל, לתת ניסיון ואתגר מקצועי לסטודנטים המסיימים ולעודד השתלבותם בתעשייה הביו-רפואית.
לפרויקטים חלק חשוב בעידוד היזמות בקרב הסטודנטים, וחלקם אף מובילים להקמת חברות הזנק ורישום פטנטים.

פרויקטים אלו מהווים נדבך מרכזי בחזון הפקולטה, לחתור לבניית גשר למצוינות ובמה לקשרים ושיתופי פעולה ארוכי טווח בין האקדמיה והחברות המובילות בתעשייה.

הפקולטה מאחלת הצלחה לסטודנטים המסיימים, ומקווה לראותם בעתיד נוטלים חלק פעיל בפרויקטים חשובים אלו כמנחים מהתעשייה.

בברכה,
פרופ' שולמית לבנברג , דיקנית הפקולטה
פרופ'מ נתנאל קורין, אחראי קורס פרויקטים

הפקולטה להנדסה ביו-רפואית

טכניון

כנס

פרויקטים

26 ביוני, 2018

תקצירים

הטכניון - מכון טכנולוגי לישראל / הפקולטה להנדסה ביו-רפואית

TECHNION – Israel Institute Of Technology / Department Of Biomedical Engineering